Imaging Transgene Expression with Radionuclide Imaging Technologies[1]

S.S. Gambhir*, H.R. Herschman*, S.R. Cherry*, J.R. Barrio*, N. Satyamurthy*, T. Toyokuni*, M.E. Phelps*, S.M. Larson[†], J. Balatoni[†], R. Finn[†], M. Sadelain[†], J. Tjuvajev[†] and R. Blasberg[†]

*UCLA School of Medicine; [†]Memorial Sloan-Kettering Cancer Center

Abstract

A variety of imaging technologies are being investigated as tools for studying gene expression in living subjects. Noninvasive, repetitive and quantitative imaging of gene expression will help both to facilitate human gene therapy trials and to allow for the study of animal models of molecular and cellular therapy. Radionuclide approaches using single photon emission computed tomography (SPECT) and positron emission tomography (PET) are the most mature of the current imaging technologies and offer many advantages for imaging gene expression compared to optical and magnetic resonance imaging (MRI)-based approaches. These advantages include relatively high sensitivity, full quantitative capability (for PET), and the ability to extend small animal assays directly into clinical human applications. We describe a PET scanner (microPET) designed specifically for studies of small animals. We review ''marker/reporter gene'' imaging approaches using the herpes simplex type 1 virus thymidine kinase (HSV1-tk) and the dopamine type 2 receptor (D2R) genes. We describe and contrast several radiolabeled probes that can be used with the HSV1-tk reporter gene both for SPECT and for PET imaging. We also describe the advantages/disadvantages of each of the assays developed and discuss future animal and human applications. *Neoplasia* (2000) **2**, 118–138.

Background

The increasing knowledge of the genetics and molecular biology of human disease, particularly in human cancer [1], has led to the application of new biologic approaches in therapy. A limitation of many biologic-based therapies has been our inability to achieve controlled and effective delivery of biologically active molecules to tumor cells or their surrounding matrix. This condition is particularly limiting for biologically active compounds that have very short biologic half-lives and exhibit site-specific therapeutic and toxic effects. Gene-based therapy can provide control over the level, timing and duration of action of these biologically active products by including specific promoter/activator elements in the genetic material transferred, resulting in more effective therapeutic interventions. Methods are actively being developed for controlled gene delivery to various somatic tissues and tumors using novel formulations of DNA, and for controlling gene expression using cell specific, replication-activated, and drug-controlled expression systems [2].

Current gene-based therapies for cancer involve several different biologic approaches to treatment. Moreover, new approaches continue to be developed. There are over 150 human gene-therapy clinical trials currently being investigated in the USA [3], and additional studies are being performed in Europe and Asia. There are over 25 "gene marker" protocols that are primarily designed to assess the efficacy and safety of gene transfer and gene therapy in patients. Most of these protocols involve transfer of the neomycin resistance gene into lymphocytes or stem cells *ex vivo* and their re-administration to patients. Questions related to the distribution and persistence of the genetically altered cells, identified by their resistance to neomycin toxicity, are being addressed. There are also over 20 "drug sensitivity" protocols, most of which involve retroviral transfer of the herpes simplex virus type 1 thymidine kinase marker/reporter gene (HSV1-tk) into tumor cells followed by systemic treatment with the pro-drug ganciclovir (GCV). This approach is based on the fact that certain genes can be

used to "sensitize" cells to drugs that are normally inactive or nontoxic (e.g., pro-drug). These genes have been termed "susceptibility" or "suicide" genes. Their use in cancer therapy is to create significant differences between normal and malignant cells by selective expression of the "suscept-ibility" gene in malignant, but not normal cells. For example, herpes simplex type 1 virus thymidine kinase enzyme (HSV1-TK) selectively converts the normally non-toxic pro-drug, GCV, into toxic compounds that results in cell death [4]. *Note that HSV1-tk refers to the gene and HSV1-TK refers to the enzyme.* A non-invasive, clinically applicable method for quantitatively imaging the expression of successful gene transduction in target tissue or specific organs of the body would be of considerable value; it would facilitate the monitoring and evaluation of gene therapy in human subjects by defining the *location(s)*, *magnitude* and *persistence* of gene expression over time.

Two different strategies can be used to image "therapeu-tic" transgene expression. The first approach involves *direct* imaging of "therapeutic" transgene expression using a probe that is specific for and accumulates in proportion to the level of gene product expressed in transduced/transfected tissue. For example, anti-cancer gene therapy using *HSV1-tk* and GCV can be coupled with imaging of the accumulation of radiolabeled probes that are selectively phosphorylated by HSV1-TK in transduced/transfected tissue. This is an example of a direct imaging approach, and the direct imaging strategy is described in greater detail in a later section. A second approach involves *indirect* imaging of "therapeutic" transgene expression using a marker/reporter gene coupled to most any "therapeutic" transgene of choice. This strategy requires proportional and constant co-expres-sion of both the marker/reporter gene and the "therapeutic" gene over a wide range of transgene expression levels. An advantage of this approach is that it provides for a much wider application of "therapeutic" transgene imaging, be-cause it is coupled to well-established marker/reporter gene imaging paradigms (such as *HSV1-tk*). Namely, a specific probe and imaging paradigm does not have to be developed and validated for each "therapeutic" transgene. The ad-vantages and limitations of an indirect imaging strategy are also described in greater detail in a later section.

A schematic for imaging marker/reporter gene expres-sion is shown in Figure 1. This transgene imaging paradigm is independent of a particular vector; namely, it can be used with any of the several currently available vectors (e.g., retrovirus, adenovirus, adeno-associated virus, lentivirus, liposomes, etc.). The common feature for all vectors is the cDNA expression cassette containing the transgene(s) of interest. The arrangement of the expression cassette can be varied and the transgene(s) can be driven by any promoter of choice. The promoter can be constitutive, leading to continuous transcription or can be inducible, leading to controlled expression. The promoter can also be cell-specific, allowing expression of the transgene to be restricted to certain cells. The transgene can encode for 1) an enzyme (e.g., HSV1-TK) that leads to trapping of a radiolabeled probe or 2) an intracellular and/or extracellular receptor

(e.g., D2R) that would lead to partially reversible or irreversible binding of a radiolabeled ligand. In the next section, we describe properties of an ideal marker/reporter gene and marker/reporter probe. Instrumentation for radio-nuclide-based imaging approaches are also described. We then describe the *HSV1-tk* and D2R marker/reporter gene systems in detail. Finally, we discuss animal and human applications of the marker/reporter genes developed to date.

Characteristics of a Good Marker/Reporter Gene and Marker/Reporter Probe

Clinical monitoring of gene expression requires the appropriate *combination* of *marker/reporter transgene* and *marker/reporter probe*. We consider the following character-istics to be ideal, if not essential [5,6]. 1) A marker/reporter transgene is usually a "foreign gene" that is not present (or
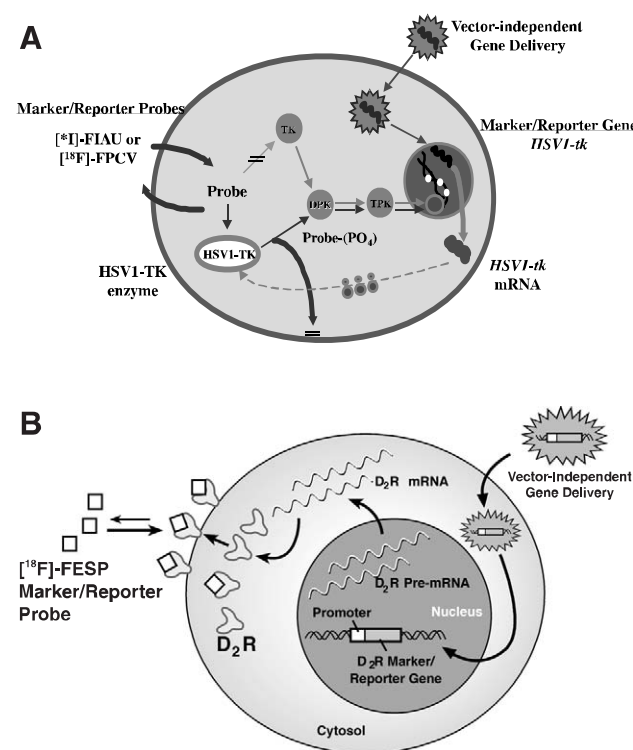
Figure 1. *(A) Schematic for imaging HSV1-tk marker/reporter gene expression with marker/reporter probes 5-iodo-2'-fluoro-2'deoxy-1-β-D-arabino-furanosyl-uracil (FIAU) or 8-[^18^F]fluoropenciclovir (FPCV). The HSV1-tk gene complex is transfected into target cells by a vector, which could be a retrovirus, an adenovirus, a liposome or any other transfer vector. Inside the transfected cell, the HSV1-tk gene is transcribed to HSV1-tk mRNA and then translated on the ribosomes to the protein enzyme, HSV1-TK. After FIAU or FPCV phosphorylation by the HSV1-TK enzyme, the radiolabeled marker/reporter probes do not readily cross the cell membrane and are "trapped" within the cell. Thus, the magnitude of marker/reporter probe accumulation in the cell reflects the level of HSV1-TK enzyme activity and level of HSV1-tk gene expression. FIAU-PO_4 is incorporated into the DNA of dividing cells, whereas FPCV-PO_4 and other phosphorylated acycloguanosine compounds act as DNA chain terminators and DNA polymerase inhibitors. (B) Schematic for imaging D2R marker/reporter gene expression with the marker/reporter probe 3-(2'-[^18^F]fluoroethyl)-spiperone (FESP). The dopamine type 2 receptor (D2R) marker/reporter gene once delivered to a cell by a vector of choice is transcribed to D2R mRNA and then translated to D2R. FESP can bind to extracellular and intracellular D2R receptors leading to probe accumulation in cells expressing D2R. Levels of accumulation of FESP reflect the level of D2R gene expression.*

not normally expressed) in the host tissue, and the gene product is an enzyme or receptor that can be expressed in transduced or transfected host cells. The enzyme or receptor must be non-toxic to host cells and lead to accumulation of the reporter probe within transduced or transfected cells. The enzyme or receptor should also not significantly perturb normal cell function. 2) A marker/reporter probe is chosen to match the marker/reporter transgene; it is a compound that is not metabolized (or only slowly metabolized) by the host, and does not accumulate in host tissues that do not express the marker/reporter gene. The probe can be radiolabeled with appropriate isotopes for clinical imaging using gamma camera, single photon emission computed tomography (SPECT), or positron emission tomography (PET) techniques. 3) The marker/reporter probe must cross cell membranes readily for an enzyme or intracellular receptor, be rapidly metabolized or bound by the marker/reporter gene product and be effectively trapped within transduced or transfected cells throughout the period of imaging, and it must accumulate to levels that are measurable by existing clinical imaging techniques. 4) The accumulation of the "probe" in transduced or transfected cells must reflect the activity of the marker/reporter transgene product and thereby, the expression of the marker/reporter transgene in transduced or transfected tissue. Further details for an ideal marker/reporter gene imaging assay are described elsewhere [5,6].

It is important to note that radionuclide-based methods offer some unique advantages over optical (reviewed in Ref. [7]) and magnetic resonance imaging (MRI) (reviewed in Ref. [8])-based approaches for imaging marker/reporter gene expression. Radionuclide-based methods offer the highest level of sensitivity for imaging relatively low levels of marker/reporter gene expression. SPECT and PET techniques are able to image as low as 10^{-10} to 10^{-12} M of radiolabeled substrate. As relatively weak promoters are used, and transcription of DNA leads to relatively low levels of mRNA and protein, it is important to have imaging methods that are highly sensitive. Furthermore, the radionuclide-based methods offer the unique advantage of being highly quantitative. PET allows for the quantitation of absolute levels of radionuclide probes, and through the use of tracer kinetic modeling and dynamic imaging, rate constants representing underlying biochemical processes can be obtained (reviewed in Ref. [9]). Another advantage of radionuclide-based approaches (that is not currently possible with optical imaging) is the ability to move from animal models into direct human applications with existing clinical scanners.

Radionuclide Imaging Instrumentation

Radiotracer imaging technologies that can measure the distribution of radiolabeled tracers in the human body are widely available and have a wide range of clinical and research applications. Two classes of clinical nuclear imaging systems exist—those designed to imaging single-gamma emitting radionuclides such as Technetium-99m or

Iodine-131 and those designed to image positron-emitting radionuclides such as Fluorine-18, Carbon-11, Nitrogen 13, Oxygen-15 and less often Copper-64 and Iodine-124. The former is known as single photon imaging, or when performed tomographically, SPECT. The latter is known as PET. In general, PET has higher spatial resolution and sensitivity, and is easier to quantify than SPECT; however, at this time, SPECT systems are more widely available in the clinical setting. Newer hybrid systems that will perform both PET and SPECT are also now commercially available.

The desire to image mouse models of human disease has led to rapidly increasing interest and efforts in developing imaging technologies that can measure the distribution of radiolabeled tracers in vivo in the mouse [10]. Autoradiography is a well-established technique that requires sacrificing the animal of interest [11], and placing tissue slices in direct contact with analog or digital film. Although autoradiography is invasive, it allows for the use of various isotopes including beta-emitters (e.g., Carbon-14) that cannot be used with PET/SPECT. Digital whole body autoradiography (DWBA) provides an ideal high-throughput environment for testing various tracers in vivo or for verifying with greater anatomic delineation the results obtained after non-invasive imaging approaches such as PET [12]. A resolution as high as 25 μm can be obtained with DWBA and results can be obtained in relatively short time periods of 4 to 72 hours. Although autoradiography has and continues to play a key role, noninvasive approaches are highly desirable for many applications. For applications in which the same animal needs to be repeatedly followed, or for applications in which it is too expensive to study large sets of animals at various time-points of the study, a non-invasive approach is desirable. Furthermore, for human applications, although tissue biopsies can be performed, a whole-body image is often desirable because the entire body can be sampled through a single procedure.

In essence, the goal for radionuclide-based imaging instrumentation has been to develop an in vivo analog of autoradiography. The development of assays for imaging gene expression in living animals places special demands on the imaging technology. For both PET and SPECT, the goal has been to develop nuclear imaging systems with sufficient spatial resolution to resolve the structures of interest in a mouse, and with sufficient sensitivity that high signal-to-noise images can be obtained without requiring the marker/reporter probe to exceed the mass limits of a tracer. A further concern is related to cost, and the ability to make this technology widely available. This section focuses on the developments in small animal PET imaging. Although less well developed at this time, it should be noted that there is also considerable activity in developing small animal systems that image single-photon emitters [13,14].

A growing realization of the potential power of PET in animal research, together with several technological innovations has led to the development of dedicated animal PET scanners by a number of research centers in the past 5 years. The first system designed specifically for rodent imaging was the RAT-PET system developed at Hammer-

smith Hospital [15]. Although this system made use of relatively large scintillation detectors (identical to those used in many clinical PET scanners), and was therefore limited to a resolution in the 3 to 4 mm range, it did establish the principle of small animal imaging with PET. RAT-PET, despite its relatively coarse spatial resolution, clearly demonstrated the ability of PET to obtain relevant biologic information from the dopaminergic system of the rat using highly specific radiotracers [16,17]. These results encouraged a number of research groups worldwide to develop very high-resolution PET systems, with a focus on the opportunities afforded by the sophistication of genetic manipulation techniques in the mouse [18–22].

One example of a dedicated small animal PET system is the microPET system [18], developed at UCLA specifically to meet the needs of the new assays being developed for imaging gene expression. The microPET scanner, shown in Figure 2, consists of 30, high-resolution, fiber-optically coupled lutetium oxyorthosilicate scintillation detectors arranged in a 17-cm-diameter ring. Each detector is readout by a 64-element multi-channel photomultiplier tube. The detectors and electronics are mounted inside a gantry measuring 90 cm wide by 140 cm high. The animal port is 16 cm in diameter. The transverse field of view is 11 cm and the axial field of view is 1.8 cm. There is also a computer-controlled bed allowing the whole body of the mouse to be scanned through the system. microPET has a reconstructed image resolution of 1.8 mm in all three axes (volumetric resolution = 0.006 ml) and an absolute sensitivity of 5600 cps/MBq (250 keV lower energy threshold) at the center of the field of view [23]. The volumetric resolution is more than an order of magnitude better than state-of-the art clinical PET systems. Since microPET became fully functional in summer 1997, over 1600 studies small animal studies have been successfully completed using a range of Fluorine-18-
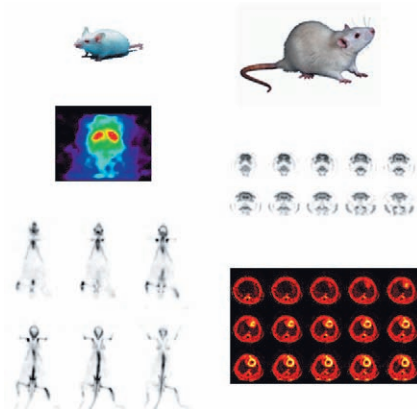

Figure 3. *Examples of microPET images. Left column (mice images): (top) $[^{11}C]$-carfentanil binding to striata in mouse brain; (bottom) $[^{18}F]$-fluoride mouse bone scan. Right column (rat images): (top) $[^{18}F]$fluorodeoxyglucose (FDG) coronal images of rat brain; (bottom) FDG transverse sections at level of rat myocardium.*

and Carbon-11-labeled radiotracers. The system has been demonstrated to be fully quantitative, both in phantom studies and in direct correlation with autoradiographic studies of the rat brain. User-friendly data acquisition and image reconstruction software to support a wide range of studies, specifically high-resolution, whole-body imaging of mice, has also been developed. Volumetric images can be reconstructed using analytic algorithms [24], or by using more sophisticated statistical algorithms that accurately model the physics and geometry of the imaging system, and the statistics of the data collection process [25]. Examples of microPET images of a mouse and rat injected with various tracers are shown in Figure 3.

The latest generation of small animal PET scanners, of which microPET is an example, is clearly demonstrating the potential of PET imaging technology in studying animal models of human disease. Nowhere is the contribution more apparent than in merger of modern molecular biology techniques with PET imaging in transgenic mice and in the development of novel gene therapy strategies. While great progress has been made in the past 5 years, it is also clear that animal PET technology is still in its infancy and that we are still a long way from reaching the resolution and sensitivity limits imposed by geometrical considerations and the physics of the positron annihilation process. We can therefore predict that the performance of animal PET scanners is likely to improve substantially in the next few years and will be accompanied by a reduction in both the size and cost of the scanners. Once the first commercial systems become available in the year 2000, this technology is likely to spread quickly throughout research centers with active PET research programs. There is also potential for animal PET imaging beyond the confines of traditional PET imaging centers, particularly in the areas of molecular biology and pharmacology. Although the issue of tracer availability still needs to be addressed, it is important to note that a majority of the world's major research institutions have biomedical cyclotrons or are within close proximity to one. Furthermore, small companies that can supply positron-labeled radio-

Figure 2. *MicroPET scanner developed at UCLA for high-resolution PET imaging of small animals. Shown is the first-generation microPET scanner. The scanner has a transverse field of view of 11 cm and an axial field of view of 1.8 cm. The spatial resolution of the scanner is ~1.8³ mm³. An entire mouse can be scanned using multiple bed positions in 30 to 60 minutes. Newer versions of this scanner will allow for ~1³ mm³ spatial resolution and scanning times for an entire mouse in under 10 minutes.*

pharmaceuticals to various parts of the country already exist and are rapidly growing. The next few years will bring many exciting challenges as the potential applications for this technology are explored in depth.

Herpes Simplex Virus Type 1 Thymidine Kinase Marker/Reporter Gene

HSV1-TK, like mammalian TKs, phosphorylates thymidine (TdR). Unlike mammalian TKs, HSV1-TK has relaxed substrate specificity and phosphorylates acycloguanosines (e.g., acyclovir, ACV; GCV; penciclovir, PCV) as well as TdR analogues (e.g., FIAU) (see Figure 4). Cellular enzymes then convert acycloguanosine monophosphates
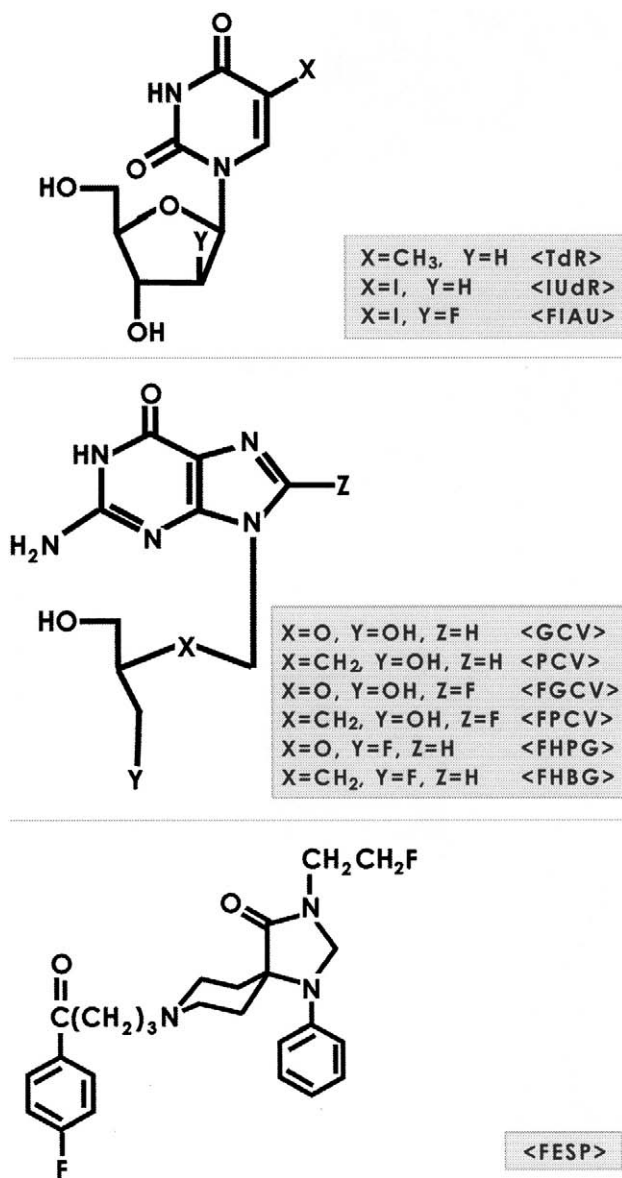

Figure 4. *Chemical structures for marker/reporter probes for HSV1-TK and D2R. Derivatives of thymidine as substrates for HSV1-TK (top panel), derivatives of acycloguanosine as substrates for HSV1-TK (middle panel), and FESP as a ligand for D2R (bottom panel). Abbreviations are as stated in the main body of the paper.*

Table 1. Comparison in *Cell Culture* of the Sensitivity and Selectivity of Three Substrates for HSV1-TK.

Probe	Sensitivity*	Selectivity[†]	n
FIAU	0.0083 ± 0.0013	0.204 ± 0.042	16
Ganciclovir	0.00039 ± 0.00015[‡]	0.218 ± 0.071	3
IUdR	0.0019 ± 0.0024[‡]	0.006 ± 0.001[‡]	3

n, number of concurrent RG2TK+ and RG2 experiments.
*Sensitivity is defined as Δ(Probe/TdR uptake ratio)/Δ(HSV1-TK mRNA/S28 RNA IOD) and is a measure of the ability of a given probe to detect cells that express *HSV1-TK*. [†]Selectivity is defined as sensitivity/(Probe/TdR uptake ratio) for RG2 cells and is a measure of the ability of a given probe to distinguish cells that express the *HSV1-tk* gene from control (wild-type) cells. Note that other probes (e.g., penciclovir) have not been compared in this manner.

and the monophosphate of FIAU to di- and triphosphates, which— if present in sufficient concentration— kill cells by incorporation as chain-terminating derivatives and/or by inhibition of DNA polymerase.

HSV1-tk has been extensively studied; it is non-toxic in humans and is currently being used as a "susceptibility" gene (in combination with GCV) in clinical gene therapy protocols. *HSV1-tk* can be used as a marker/reporter gene as well as a therapeutic gene [26–29]. In gene therapy protocols using *HSV1-tk* as a susceptibility gene, identifying the location and magnitude of HSV1-TK expression by noninvasive imaging would provide a highly desirable measure of expression (following successful gene transfection) and provide a basis from which the timing of GCV treatment can be optimized. This represents an ideal situation where the therapeutic and marker/reporter genes are the same, and is an example of a direct imaging approach.

Analogues of TdR as Marker/Reporter Probes for the HSV1-tk Marker/Reporter Gene

Initial work at MSKCC studied three compounds (FIAU, iododeoxyuridine [IUdR] and GCV) (Figure 4) as potential marker/reporter probes for imaging *HSV1-tk* gene expression, using a cell culture model [5]. FIAU was included in these initial studies because of its previous use as a potential anti-viral agent, and because FIAU had previously been radiolabeled for use as a viral infection imaging agent [30–34]. Of these three compounds, FIAU was considered to have good imaging potential because of its *in vitro* HSV1-TK sensitivity and selectivity characteristics (Table 1). FIAU can be radiolabeled with several different radionuclides, including Carbon-11, or no-carrier-added Iodine-131, Iodine-123 and Iodine-124, appropriate for clinical imaging with PET or SPECT.

An important characteristic of the 2'-fluoro substitution on the arabinose or ribose is that it provides a protective group against enzymatic cleavage of the N-glycosidic bond by nucleoside phosphorylases. The increased stability of the N-glycosidic bond results in a significant prolongation of plasma half-life of these compounds and they are excreted largely unchanged in the urine. As a result, a greater amount of non-degraded radiolabeled drug is delivered to the target tissues and confounding problems associated with imaging radio-

labeled metabolites in both target and surrounding tissue are avoided.

On the basis of the sensitivity and selectivity indices obtained in cell culture (Table 1) [5] and the availability of 2-[^{14}C]FIAU, testing was performed to determine if there is a consistent relationship between the level of *HSV1-tk* expression in different *HSV1-tk* transduced cell lines and the level of FIAU accumulation. Several RG2TK clones, as well as wild-type RG2 and bulk culture RG2TK+ cells, were compared with respect to FIAU accumulation and two independent measures of *HSV1-tk* expression: a) sensitivity to the anti-viral drug GCV, a functional measure of *HSV1-tk* expression (50% inhibitory concentration, IC$_{50}$) and b) normalized integrated optical density (IOD) values of *HSV1-tk* mRNA identified on Northern blot analysis. Accumulation of FIAU, expressed as the FIAU/TdR uptake ratio, was proportional to the levels of *HSV1-tk* mRNA in corresponding cell lines, and as expected, a highly significant inverse relationship was also observed between FIAU uptake and GCV sensitivity [5]. Additional cell lines, including W256 tumor cells, were transduced with the STK and STLEO retroviruses (containing *HSV1-tk*). Following the transductions, clonal cell lines were derived from the bulk culture and were shown to express different levels of *HSV1-tk*. The level of FIAU accumulation in each of the cell lines was compared to their sensitivity to GCV (an independent assay of *HSV1-tk* expression) (Figure 5). These results demonstrate a consistency between FIAU accumulation and GCV sensitivity that is independent of cell line or transduction vector.

The first series of imaging experiments with FIAU were performed in Fisher 344 rats with intracerebral (i.c.)
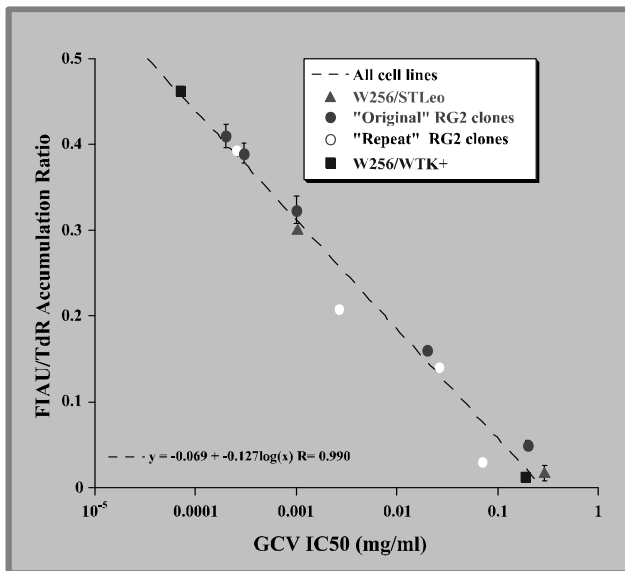

Figure 5. *Comparative assays of HSV1-tk expression. The radiotracer accumulation ratio (FIAU/TdR) that normalizes FIAU uptake for cell proliferation is compared to a functional assay of HSV1-tk expression; namely, sensitivity (IC$_{50}$) to the antiviral drug, ganciclovir. Four different sets of stably transduced cell lines (clones) expressing HSV1-tk were studied. A highly reproducible relationship between these two assays is demonstrated that is independent of cell line and retroviral transduction vector.*

RG2TK+ and RG2 tumors using quantitative autoradiography (QAR) techniques [5]. Sixteen days after RG2TK+ and RG2 cell inoculation, each animal was injected intravenously with 50 μCi of 2-[^{14}C]FIAU and killed with euthanasia solution 24 hours later. The brain was rapidly extracted and frozen in preparation for cryo-sectioning and autoradiography [35,36]. The ability to selectively image the expression of a marker/reporter gene, *HSV1-tk*, in vivo is shown in Figure 6. The histology and autoradiographic images were generated from the same tissue section (*panels A* and *B*) and registered so that all regions of interest (ROIs) drawn would outline equivalent regions on the other images. The outline of the RG2TK+ and RG2 tumors in each hemisphere of the rat brain is clearly seen in the toluidine blue-stained histologic section (Figure 6A). In the autoradiographic image (Figure 6B), the RG2TK+ tumor is clearly visualized, whereas the RG2 tumor is barely detectable and the surrounding brain is at background levels. The punctate heterogeneous levels of FIAU activity observed in the RG2TK+ tumor (excluding the white areas representing tissue necrosis) are thought to reflect differences in *HSV1-tk* gene expression in the non-clonal, mixed population of transduced RG2TK+ cells growing intracerebrally. Quantitative analysis yielded mean activities of 0.180 ± 0.140 and 0.022 ± 0.024 percentage dose per gram (%dose/g) for the RG2TK+ and RG2 tumors, respectively. Peak activity in the RG2TK+ tumor was 0.43 %dose/g; adjacent brain activity was below the level of detection (<0.005 %dose/g) on the autoradiograms.

The tissue section used for autoradiography in (Figure 6C) was adjacent to the one used in (Figure 6B); it was rinsed in acid solution (10% TCA) for 4 hours to remove non-incorporated FIAU and radiolabeled metabolites before autoradiographic exposure. Rinsing tissue sections had little effect on the distribution and amount of radioactivity measured in the autoradiogram (compare Figure 6B and C). This indicates a very low background activity due to soluble radiolabeled metabolites and demonstrates the value of using an ''in-vivo washout'' strategy (imaging 24 hours after FIAU administration) to reduce background radioactivity.

The second series of experiments with FIAU involved gamma camera imaging [37]. Subcutaneous (s.c.) implantation of 10^6 wild-type RG2 cells into both flanks of athymic Harlan-Sprague-Dawley R-Nu rats; following a 46-day growth period, the right and left flank tumors reached a 5×4×3 and 3×2×1 cm^3 size, respectively. The larger left-sided tumor was inoculated with 10^6 gp-STK-A2 vector-producer cells (retroviral titer: 10^6 to 10^7 cfu/ml, cfu=colony forming units) in 100 μl of minimum essential medium (MEM) (without fetal calf serum or FCS) to induce in vivo transfection and transduction of the tumor. Fourteen days after gp-STK-A2 cell inoculation, no carrier added [^{131}I]FIAU was prepared and 2.8 mCi was injected intravenously into the animal (that previously received a thyroid blocking dose of NaI). Gamma camera imaging was performed at 4, 24 and 36 hours post [^{131}I]FIAU injection with a dual-headed ADAC Genesys gamma camera
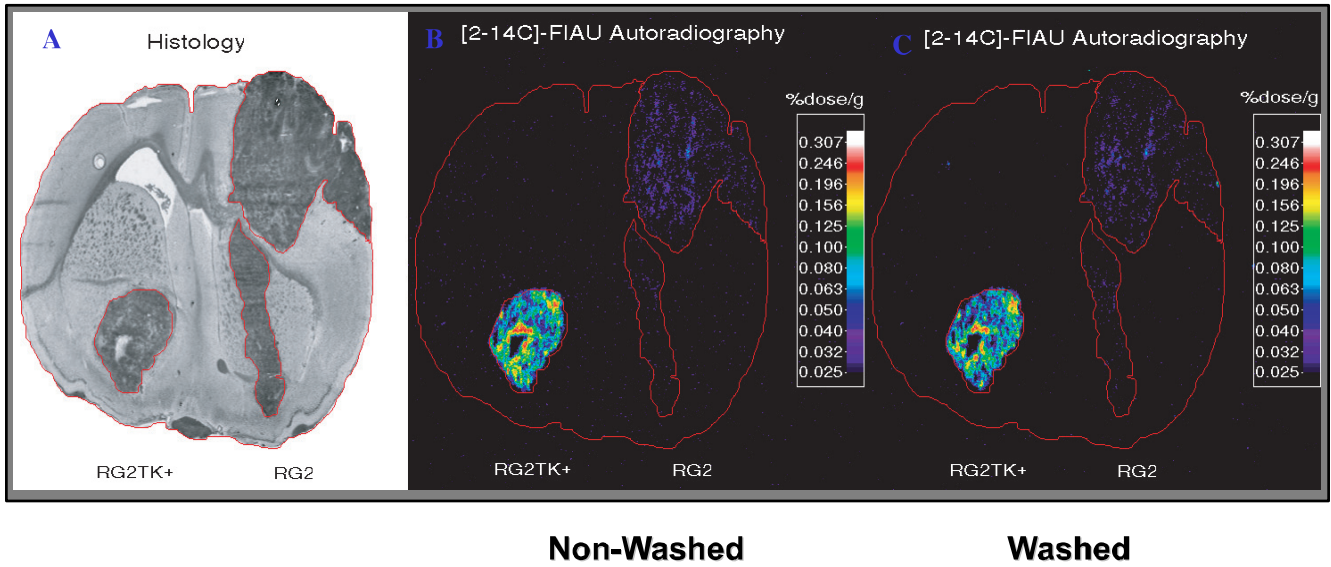
24 Hour Experiment

Figure 6. $[^{14}C]FIAU$ imaging in tumors with autoradiography. The histology and autoradiographic images were generated from the same tissue section (panels A and B). The HSV1-tk-transduced RG2TK+ and wild-type RG2 tumors in each hemisphere of the rat brain are clearly seen in the toluidine blue-stained histologic section (panel A). Twenty four hours after administration of $[^{14}C]FIAU$, the RG2TK+ tumor is clearly visualized in the autoradiographic image (panel B), whereas the RG2 tumor is barely detectable and the surrounding brain is at background levels. Rinsing an adjacent tissue section for 4 hours in 10% TCA had little effect on the distribution and amount of radioactivity measured in the autoradiogram (compare panels B and C).

(Milpitas, CA) equipped with a high-energy, high-resolution collimator. The images have been normalized to a reference standard (not shown in the field of view) to account for differences in counting time (10-, 15- and 20-minute periods, respectively) and decay, and can be compared to a scaled photographic image of the animal (arrow indicates the site of inoculation of vector producer cells into the tumor; Figure 7). The normalized images demonstrate washout of radioactivity from the body with retention of activity in the area of gp-STK-A2 cell inoculation. The 24- and 36-hour

images show specific localization of retained radioactivity in the same area where the vector producer cells were injected. It should be noted that the site of gp-STK-A2 cell inoculation and *HSV1-tk* transduction of the tumor can be seen in the 4-hour image with lower intensity scaling, although background levels of radioactivity are substantially higher than in the 24- and 36-hour images. It is apparent that the area of retained radioactivity (area of transduction) was limited and did not extend throughout the tumor. The non-transduced contralateral tumor (right side) and other tissues did not show any
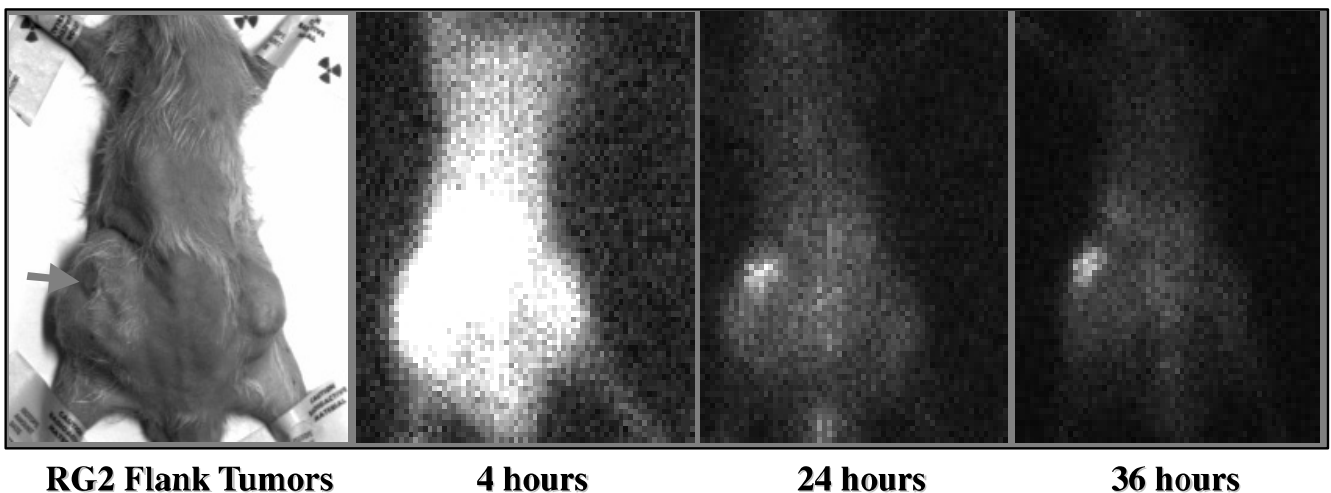
Figure 7. $[^{131}I]FIAU$ imaging of tumors with a gamma camera. Gamma camera imaging was performed at 4, 24 and 36 hours after $[^{131}I]FIAU$ injection in animals bearing bilateral RG2 flank tumors; the images have been normalized to a reference standard (not shown in the field of view). The arrow indicates the inoculation site of HSV1-tk retroviral vector producer cells (gp-STK-A2) in the left flank tumor. The images demonstrate washout of radioactivity from the body with specific retention of activity in the area of gp-STK-A2 cell inoculation (see the 24- and 36-hour images). The non-transduced contralateral tumor (right flank) and other tissues did not show any retention of radioactivity.

retention of radioactivity. These sequential images show the importance of a washout strategy and justifies delayed imaging at 24 or 36 hours after FIAU administration.

The third series of experiments performed at MSKCC involved PET imaging with [124I]FIAU [38]. Sub-cutaneous implantation of five different cell lines (5×10^6 cells in 100 μl) was performed at different sites in the same animal (including wild-type RG2 cells; a mixed population of *in vitro* transduced RG2TK+ cells; and from three single cell-derived clones: RG2TK#4, RG2TK#16 and RG2TK#32). The implantation of multiple tumors per animal provides the opportunity for a better comparison since all tumors are exposed to the same levels of [124I]FIAU in blood plasma (same input function). No carrier added [124I]FIAU was prepared and 25 to 50 μCi was injected intravenously into each animal (that previously received a thyroid blocking dose of NaI) when the tumors grew to approximately 1 to 1.5 cm in diameter (Figure 8) [38]. PET imaging was performed 32 hours after [124I]FIAU injection with a General Electric Advance PET tomograph. The PET acquisitions were obtained over 40 min, in 3D (septa-out) mode. A transmission scan was performed before each emission

acquisition, and the reconstructed images were corrected for attenuation and scatter. A set of Iodine-124 reference standards of different volumes (1 to 20 ml) and different radioactivity concentrations was placed within the field of view of the PET scanner. These standards were used for quantitation of the images and to account for differences in imaging time and radioactive decay.

Radioactivity concentration (%dose/g) in tumors was also assessed by tissue sampling and by gamma spectroscopy after animal sacrifice to confirm the validity of the PET measurements. Highly specific levels of FIAU accumulation (>0.1 %dose/g) were observed in the areas of the RG2TK+, RG2TK#4 and RG2TK#16 tumors. RG2 wild-type tumors and tumors derived from the low-expressor clone (RG2TK#32) showed no substantial accumulation above background radioactivity (<0.01 %dose/g). There was a reasonably good correlation between the levels of [124I]FIAU-derived radioactivity (%dose/g) obtained by quantitation of the PET images and those obtained by the direct tissue sampling and gamma spectroscopy (slope = 0.95, $r = 0.52$). The comparison between the PET and well counter measurements was better for the higher-activity
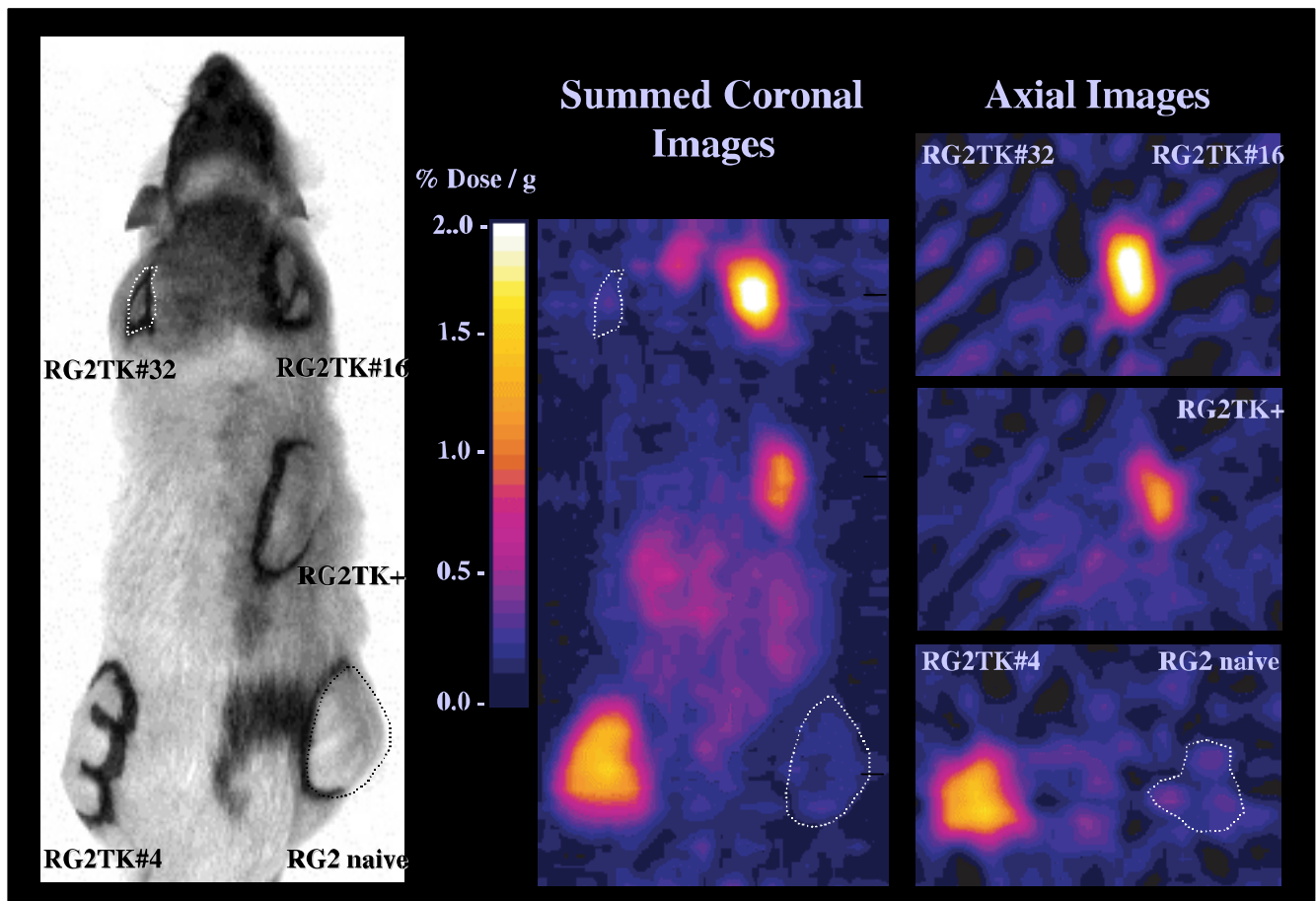
Figure 8. *[124I]FIAU PET images of HSV1-tk gene expression. Imaging multiple tumors (produced from stably transduced cell lines expressing different levels of HSV1-tk) in the same animal provides direct image and quantitative comparisons, since all tumors are exposed to the same levels of [124I]FIAU in the blood (same input function). PET imaging (over 40 min in 3D, septa-out mode) was performed 32 hours after [124I]FIAU injection with a General Electric Advance PET tomograph (Milwaukee, WI). Note the different levels of radioactivity (%dose/g) in the tumors. The relationship between radioactivity concentration (%dose/g) in the tumors and two independent assays of HSV1-tk expression in the cell lines used to produce the tumors is shown in Figure 9.*

RG2TK+ tumor clones than the low-activity clone RG2TK#32 and wild-type RG2 tumors.

Sequential blood samples were obtained in these animals and plasma radioactivity (%dose/ml) was plotted against time following [^{124}I]FIAU administration. The kinetics of [^{124}I]FIAU elimination from blood was bi-exponential. The initial arterial plasma clearance half-time of [^{124}I]FIAU was 1.1 hour; the second clearance half-time was 4.4 hours. The 32-hour tissue radioactivity measurements were normalized to the plasma concentration time course (input function) to obtain tissue uptake constants, K_i. The K_i is a measure of net blood-to-tissue uptake (blood clearance constant); it normalizes the observed tissue counts for the blood input function [39,40]. The range of [^{124}I]FIAU accumulation, expressed as K_i in RG2TK+, RG2TK#4 and RG2TK#16 tumors varied from 0.375 ± 0.071 to 1.03 ± 0.325 μl/min per gram. In the RG2TK#32 (the low-expressor clone) and wild-type RG2 tumors, the K_i values were substantially lower, 0.028 ± 0.008 and 0.034 ± 0.009 μl/min per gram, respectively.

To further assess whether PET imaging of the *HSV1-tk* gene expression in transduced tumors reflects the level of *HSV1-tk* gene expression, comparisons of levels of [^{124}I]FIAU accumulation measured at 32 hours (%dose/g) and the FIAU incorporation constant (K_i) to two independent measures of *HSV1-tk* expression in the cell lines that were used to generate these tumors were performed. Highly significant relationships were observed between the level of [^{124}I]FIAU accumulation (%dose/g or K_i) and *HSV1-tk* mRNA levels as well as the sensitivity (IC$_{50}$) of corresponding cell lines to the antiviral drug, GCV

(Figure 9). The slope of the relationships in Figure 9 constitute a "sensitivity index" for the FIAU-PET image, and this slope can be used to generate a color-coded scale bar for a parametric image that reflects GCV sensitivity (IC$_{50}$) of the tumors [38].

Issues about potential toxicity associated with the administration of radiolabeled $2'$-fluoro nucleosides for diagnostic studies in patients have been raised [37]. This concern relates to the serious complications and two deaths that were associated with a clinical trial evaluating the long-term administration of FIAU as a potential anti-viral agent in treatment of patients with chronic hepatitis-B virus infection [41] and to the ethics of administering tracer doses of FIAU and other $2'$-fluoro nucleoside radiopharmaceuticals to patients for diagnostic purposes. To appreciate the significance of these issues, the difference between a therapeutic dose of FIAU administered in clinical trials and an equivalent dose administered for diagnostic imaging studies must be clearly understood. It should be noted that a no carrier-added procedure for radioiodination of FIAU (and other $2'$-fluoro nucleosides) has been developed [42] and was the radiosynthetic procedure used for labeling FIAU in the MSKCC studies [43]. The mass of radiopharmaceutical produced from a no carrier-added synthesis is usually very small and the specific activity of the product is usually not determined in accepted radiopharmaceutical practice. However, the theoretical specific activity of a no carrier-added synthesis can be calculated and the mass of administered radiopharmaceutical determined from the specific activity (Ci/mole), the dose of radioactivity (Ci) administered, and the molecular weight (g/mole) of the radiopharmaceutical.

A

B
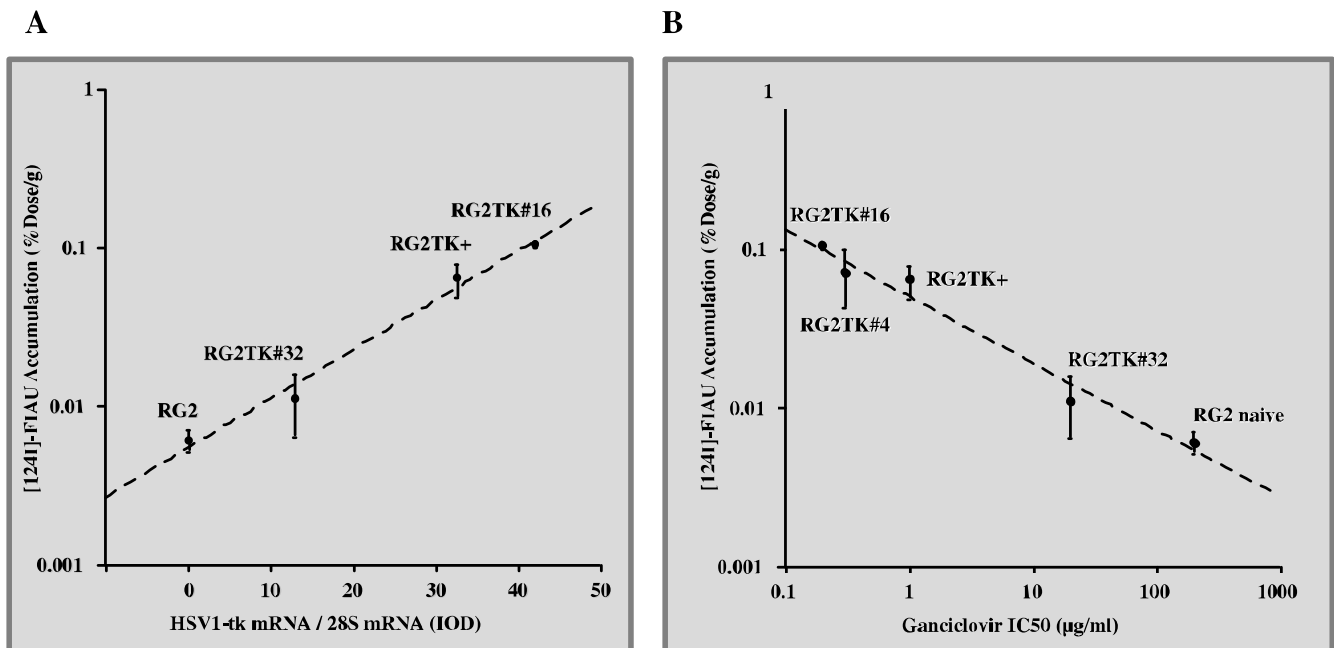
Figure 9. *Quantitative relationships between the FIAU radioactivity (%dose/g) and two independent assays of HSV1-tk expression. The FIAU radioactivity (%dose/g) data were obtained from imaging experiments shown in Figure 8. Highly significant relationships were observed between the level of [^{124}I]FIAU accumulation (%dose/g) and HSV1-tk mRNA levels (y = 0.005×e$^{(0.071x)}$, r = 0.993; left panel), and between the level of [^{124}I]FIAU accumulation (%dose/g) and sensitivity (IC$_{50}$) to the antiviral drug, GCV (y = 0.050×x$^{(-0.422)}$, r = 0.974; right panel).*

The calculated mass of a 148 MBq (4 mCi) dose of no carrier-added [124I]FIAU proposed for PET imaging studies in patients is only 47 ng (125 pmol); for a 1.1 GBq (30 mCi) dose of no carrier-added [123I]FIAU proposed for SPECT imaging studies, the equivalent mass of FIAU that would be administered is only 32 ng (85.5 pmol). A dose of 47 ng of FIAU represents only 1/75,000 to 1/2,530,000 of the daily dose (4.7×10^{-7} to 2.8×10^{-8} of the total dose) that was administered to patients in the 14- to 28-day hepatitis B clinical trials, where no FIAU-related toxicity was observed [41]. Only in the 168th day clinical trial (H3X-PPPC) did severe liver, pancreatic and neurotoxicity appeared [44].

The feasibility of imaging HSV1-TK expression in cancer patients undergoing combined HSV1-tk-GCV gene therapy with PET or SPECT has been evaluated [45]. Successful imaging will depend on several factors: 1) the level of HSV1-TK expression in the transduced tissue to be imaged; 2) the "sensitivity" and "selectivity" of the marker probe; 3) the administered dose and clearance of the marker from the blood; 4) the sensitivity of the imaging equipment; and 5) scan duration. For "clinically relevant" levels of HSV1-TK expression in transduced/transfected tumor tissue, the radioactivity concentration of [124I]FIAU in the transduced/transfected tumor tissue 24 hours following a 4 mCi dose was calculated to be ~0.14 to ~0.24 μCi/ml [45]. This is *~110 and ~500 times higher* for septa-in and septa-out PET acquisitions, respectively, than the lower-limit sensitivity of current (GE and Siemens) PET tomographs. For [131I] and [123I]FIAU SPECT acquisitions following a 10- and 30-mCi dose of FIAU, respectively, we estimate a count rate that is ~5 and ~10-fold above the lower-limit sensitivity of the SPECT tomograph.

Acycloguanosine Marker/Reporter Probes for HSV1-tk Marker/Reporter Gene Imaging

At UCLA, one of the approaches developed to image marker/reporter gene expression also relies on the HSV1-tk marker/reporter gene, but uses acycloguanosine (e.g., radiolabeled GCV/PCV) derivatives as marker/reporter probes [12,46] (Figure 4). The choice of acycloguanosines as potential probes was based on their ability to be radiolabeled with Fluorine-18, allowing PET imaging of HSV1-tk gene expression. Dr. Barrio et al. at UCLA had investigated fluorination of ACV in the 1980s as a potential probe for imaging Herpes viral infection (unpublished data). Consequently, although there was no pre-existing PET probe, there was in-house expertise on specifically radio-labeling acycloguanosines. The UCLA goals were to develop methods to repetitively image (e.g., every 6 to 8 hours if needed) HSV1-tk gene expression with microPET. Therefore, a short-lived isotope such as Fluorine-18 (half-life of 110 minutes) was investigated. A large part of the envisioned usage of the microPET was for imaging marker/reporter gene expression in mice; microPET development was started at about the same time as the UCLA gene expression projects. Because 2'-fluoro analogues (e.g., FIAU) are not easily labeled with Fluorine-18 (even though they contain a fluorine atom), the UCLA group decided to pursue acycloguanosine derivatives to develop a PET-based assay.

Initial cell culture uptake experiments were performed with 8-[18F]fluoroacyclovir [47], but only cells with relatively high levels of HSV1-tk gene expression could accumulate sufficient radiolabeled probe relative to control cells. This probe was, therefore, not pursued further. Subsequently, investigations used 8-[14C]-GCV and 8-[18F]fluoroganciclovir (FGCV) as marker/reporter probes for HSV1-TK [12,46]. A replication-defective adenovirus, Ad-CMV-HSV1-tk encoding HSV1-tk expressed under the control of the cytomegalovirus (CMV) promoter was developed along with a control adenovirus (an E1-deletion mutant). An adenoviral model for gene delivery was used because different levels of HSV1-tk expression can easily be achieved by titrating the dose of adenovirus, both in cell culture and *in vivo*. This titration approach avoids the problem of working with different stably transfected cell lines *in vivo*, and provides for rapid turn-over time, because tumors need not be grown *in vivo*. The UCLA group first characterized the properties of the viral system in cell culture. C6 rat glioma cells were infected with the Ad-CMV-HSV1-tk virus to produce C6tk+ cells and with control virus to produce C6tk− cells. Subsequently, infected cells were studied for levels of HSV1-tk mRNA (normalized to GAPDH), HSV1-TK enzyme activity, and accumulation of radioactive GCV. The C6tk+ cells demonstrated significantly more HSV1-tk mRNA and HSV1-TK enzyme than the C6tk− cells. Statistically significant accumulation of 8-[14C]-GCV in C6tk+ cells was achieved in relatively short times of 30 to 60 minutes compared with C6tk− cells [46].

The UCLA group then studied the accumulation of the reporter/marker probes, following adenoviral-mediated HSV1-tk delivery in mice, using DWBA. When adenovirus is injected into the tail-vein of mice, the predominant site of infection is the liver in large part due to the presence of coxsackie and adenoviral receptors (CAR) on hepatocytes. Studies were performed by injecting adenovirus into the tail vein followed by injection of 8-[14C]-GCV 48 hours later. One hour after injection of 8-[14C]-GCV mice were sacrificed and the liver assayed for levels of mRNA, TK enzyme and Carbon-14. Studies using increasing levels of Ad-CMV-HSV1-tk (0.5 to 1.0×10^9 plaque forming unit or pfu) demonstrated that accumulation of 8-[14C]-GCV (percentage injected dose per gram (%ID/g) liver) was highly correlated ($r^2 > 0.8$) to: 1) hepatic levels of HSV1-tk mRNA (normalized to GAPDH) and 2) levels of HSV1-TK enzyme. Furthermore, biodistribution studies revealed that there was very little accumulation of GCV in tissues other than the liver. Routes of clearance of GCV included the hepatobiliary and renal systems. Note that the hepatobiliary routes of clearance do not complicate image quantitation when delayed imaging is used, and when the left liver lobe is used to avoid gall-bladder activity [46]. DWBA of mice studied with this adenoviral model revealed good contrast between the liver and surrounding tissues within 1 hour after injection of GCV. Retention of radioactivity within the gallbladder was also observed [46].
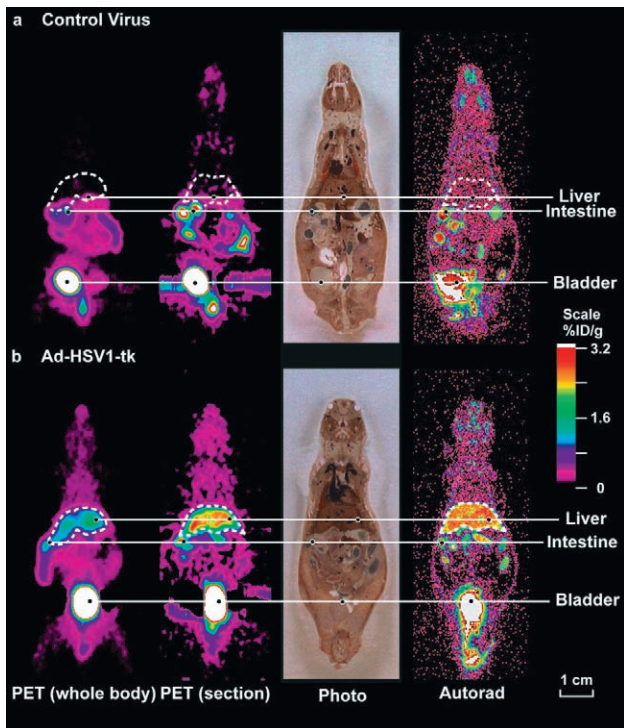
Figure 10. *MicroPET and DWBA images of mice after administration of control virus and Ad-CMV-HSV1-tk. Swiss-webster mice were injected through the tail vein with (a) 1.5×10^9 pfu of control virus or (b) 1.5×10^9 pfu of Ad-CMV-HSV1-tk virus. For each mouse, a whole body mean coronal projection image of the Fluorine-18 activity distribution is displayed on the left. The liver outline, in white, was determined from both the FGCV signal and cryostat slices. The second images from the left are coronal sections, approximately 2 mm thick, from the microPET. After their PET scans, the mice were killed, frozen and sectioned. The next images are photographs of the tissue sections (45 μm thick) corresponding to approximately the mid-thickness of the microPET coronal section. The images on the right are DWBA (autorad) of these tissue sections. The color scale represents the FGCV %ID/g tissue. Images are displayed on the same quantitative color scale, to allow signal intensity comparisons among the panels.*

As a consequence of the encouraging results obtained *in vivo* with 8-[^{14}C]-GCV using relatively short time-periods after injection, labeling of GCV with Fluorine-18 was pursued. Preparation of FGCV with specific activities of 3 to 5 Ci/mmol was made possible through new chemistry developed at UCLA [48,49]. C6 cell culture studies similar to those performed with 8-[^{14}C]-GCV were also performed with FGCV and showed significant accumulation in C6tk+ cells compared to C6tk− cells in 60 to 90 minutes [12]. Furthermore, levels of *HSV1-tk* message (normalized to GAPDH) and levels of HSV1-TK enzyme correlated well with accumulation of FGCV in C6tk+ cells. FGCV is stable *in vivo*; >98% is excreted unchanged in mouse urine in 60 min [12].

To demonstrate the ability of FGCV to image *HSV1-tk* PET reporter expression, mice were injected with control virus or Ad-CMV-*HSV1-tk*. Two days later, the mice received FGCV and were subsequently imaged with a microPET and then sacrificed and imaged using DWBA (Figure 10). Mice receiving control virus had minimal detectable hepatic activity. In contrast, mice that received Ad-CMV-*HSV1-tk* show significant FGCV liver retention. HPLC analysis of cell metabolites as well as liver extracts confirmed that FGCV had been metabolized to the mono-, di- and tri-phosphates as well as incorporated into DNA [12]. The levels of FGCV and metabolites at target tissue sites are 100-fold below pharmacological levels required for cell toxicity.

To quantitate the relationship between hepatic *HSV1-tk* expression and FGCV retention, mice were injected with varying amounts of Ad-CMV-HSV1-tk virus (0 to 2.0×10^9 pfu) and additional control virus to maintain the total viral burden at 2.0×10^9 pfu. Two days later, the mice were injected in the tail vein with FGCV and sacrificed after 180 minutes. Hepatic FGCV retention was determined by well counting. *HSV1-tk* mRNA levels and HSV1-TK enzyme levels were measured from liver samples. There is excellent correlation with the FGCV %ID/g liver for both *HSV1-tk* mRNA (r^2 = 0.81) and HSV1-TK enzyme (r^2 = 0.71) (Figure 11). When comparing 8-[^{14}C]-GCV to FGCV, there is a significant effect of fluorine in the 8 position on the ability of 8-[^{14}C]-GCV to be phosphorylated by HSV1-TK. FGCV leads to a lower sensitivity for imaging *HSV1-tk* gene expression than 8-[^{14}C]-GCV. The K_m and V_{max} measurements made at UCLA support the decreased affinity of FGCV for HSV1-TK compared to GCV by about a factor of 10 (unpublished data).
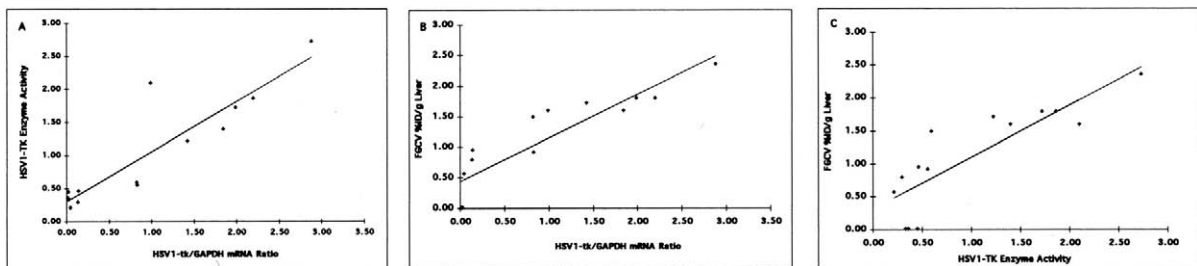
Figure 11. *FGCV retention in liver as a function of HSV1-tk gene expression. Fourteen adult swiss-webster mice were injected through the tail vein with 0 to 2.0×10^9 pfu of Ad-CMV-HSV1-tk virus and additional control virus to maintain the total viral burden to be fixed to 2.0×10^9 pfu. Forty-eight (±1) hours later, animals received a tail vein injection of FGCV. Animals were sacrificed 180 minutes later. Livers were removed and liver samples were analyzed for (i) Fluorine-18 retained in tissue; (ii) HSV1-tk mRNA levels normalized to GAPDH; and (iii) HSV1-TK enzyme levels. (Panel A) HSV1-TK enzyme levels versus HSV1-tk mRNA levels (y = 0.76x + 0.30, r^2 = 0.81). (Panel B) FGCV %ID/g liver versus HSV1-tk mRNA levels (y = 0.71x + 0.44, r^2 = 0.81). (Panel C) FGCV %ID/g liver versus HSV1-TK enzyme activity (y = 0.79x + 0.31, r^2 = 0.71). Each point represents data from a different mouse.*

To further improve the sensitivity of the *HSV1-tk* marker/reporter gene, radiolabeled PCV was also studied in cell culture [50]. PCV has been used as a pharmaceutical and is known to be cytotoxic at lower concentrations in cells expressing *HSV1-tk* compared to GCV and ACV [51]. It was reasoned that PCV would lead to a higher sensitivity of imaging *HSV1-tk* expression compared to GCV. PCV was therefore explored further. PCV leads to a two- to three-fold greater sensitivity for detecting *HSV1-tk* expression compared to GCV in cell culture and *in vivo*, utilizing the adenoviral delivery model. Recently completed studies in cell culture and *in vivo* demonstrate a two- to three-fold advantage of FPCV over FGCV. However, the fluorine in the 8-position of FPCV also decreases its affinity for HSV1-TK relative to PCV.

Several groups have studied Fluorine-18 labeled in the *sidechain* of GCV (9-[(3-[^{18}F]fluoro-1-hydroxy-2-propoxy)methyl]guanine or FHPG) [52,53] and in the *side chain* of PCV (9-[4-[^{18}F]fluoro-3-(hydroxymethyl)butyl]guanine or FHBG) [54] as an alternative to the 8-position labeling strategies previously reported by the UCLA group. The advantage of side-chain labeling is that [^{18}F]fluoride ion can be used (as opposed to [^{18}F]F$_2$ used for the synthesis of 8-[^{18}F]fluoro derivatives), and therefore high-specific activity (250 to 5000 Ci/mmol) [^{18}F]fluorinated acycloguanosines can be synthesized in relatively high yields (5 to 15 mCi). The disadvantage is that a racemic mixture results from side-chain labeling of GCV and PCV. FHPG [53,55] and FHBG [54] have been studied in cell culture models and preliminarily *in vivo*, and are also well suited for imaging *HSV1-tk* gene expression. Preliminary results support that the side-chain labeled acycloguanosine derivatives do not have decreased affinity for HSV1-TK compared to the parent compounds, unlike the observed results with the 8-position labeled acycloguanosine derivatives (UCLA, unpublished data). Studies demonstrate that these side-chain derivatives of GCV and PCV do not have any significant cell cytotoxicity at the concentrations used (UCLA, unpublished data).

The kinetics of FGCV, FPCV and FHBG have been preliminarily studied at UCLA. Each shows rapid blood clearance, with more than 95% of the initial blood activity removed in the first 30 minutes. Blood time-activity curves have been obtained for each tracer directly from images of the left-ventricle, utilizing a microPET, and compare very well to blood samples obtained from direct left-ventricular sampling. Furthermore, tracer kinetic models that help to relate the observed microPET signal for FGCV to estimates of HSV1-TK activity have preliminarily been reported [56]. Further modeling should help to better quantitate changes in transport of marker/reporter probe *versus* changes in rates of phosphorylation utilizing kinetic information obtained from the microPET.

Comparison of Alternate Marker/Reporter Probes for the HSV1-tk Marker/Reporter Gene

A detailed comparison of all the radiolabeled probes studied for imaging *HSV1-tk* marker/reporter gene expression has yet to be reported in the literature. The key confounding variable in comparing results across studies from different groups are the varying levels of *HSV1-tk* gene expression. Because different cell lines and *in vivo* models have been used, it is difficult to make an accurate comparison. However, some information already published, and new data that are emerging, provide some clues and are reviewed here.

To evaluate the proficiency of marker/reporter probes for imaging of *HSV1-tk* expression, two parameters were initially studied by the MSKCC group: 1) "sensitivity," defined as the change in probe uptake (normalized to TdR) divided by the change in *HSV1-tk* expression, and 2) "selectivity," defined as "sensitivity" divided by probe uptake due to endogenous (mammalian) TK. These two related measures were considered useful for imaging considerations because both intensity (e.g., high "sensitivity") and contrast (the ability to differentiate between HSV1-TK and endogenous-TK; e.g., high "selectivity") in the images are required. It is important to note that the "selectivity" measure should *not* be interpreted as a relative sensitivity of the probe to HSV1-TK *versus* endogenous-TK. Also, neither of the measures represents a fraction of some ideal value (i.e., they do not have a maximum of one). They are intended only for the direct comparison of different radiolabeled probes. Similarly, both measures could be correlated with marker/reporter probe accumulation in i.c. and s.c. tumors in animals; tumors produced by the same cell lines studied in tissue culture. Using the sensitivity/selectivity criteria, a comparison was published between IUdR, GCV and FIAU [5]. IUdR showed good sensitivity, but no selectivity since it is phosphorylated by wild-type cells as readily as by *HSV1-tk* transduced cells. GCV showed the best selectivity, but lower sensitivity compared to FIAU (Table 1).

The UCLA group has directly compared uptake of FGCV, FPCV, FHBG, FHPG and [^{14}C]FIAU in C6 cells expressing *HSV1-tk* compared with control C6 cells. These preliminary data in cell culture show that FIAU and FHBG are the better candidates for imaging *HSV1-tk* reporter gene expression. Studies are currently underway to confirm these results in additional cell culture models.

Although comparison of various radiolabeled probes in cell culture to determine the sensitivity and selectivity are important considerations, the true utility of alternative HSV-TK probes must ultimately be evaluated *in vivo*. Issues such as *in vivo* stability, substrate competition of various nucleoside pools, routes of clearance, and rate of cellular transport all come in to play *in vivo*. Furthermore, the specific radioisotope used will have an effect, because not all decays from a given isotope will lead to measurable event. For example, for PET studies, Iodine-124 has a positron yield of only ~23%, whereas Fluorine-18 has a positron yield of >95%. Future studies that directly compare acycloguanosines and TdR analogues *in vivo*, under equal levels of *HSV1-tk* gene expression, will help to better define the advantages and disadvantages *in vivo* for each probe. It is likely that for some applications, a radioiodine-labeled approach with FIAU will be preferable, whereas for other

applications, a fluorine-labeled approach with an acyclo-guanosine (e.g., FHBG) will be more advantageous. A key advantage for all the radionuclide approaches described over MRI-based approaches is that *tracer* levels (10^{-9} to 10^{-12} M) are used and therefore do not perturb the cell steady-state.

Mutant HSV1-tk Marker/Reporter Gene Approaches

The UCLA group has also investigated mutant *HSV1-tk* reporter genes, to further enhance the sensitivity of the *HSV1-tk* reporter assays [57]. As described above, one can develop better substrates for HSV1-TK to improve the assay sensitivity. Alternatively, because a marker/reporter gene has to be introduced into the system of interest, one can develop *a priori* a marker/reporter enzyme that is optimized for a given marker/reporter probe. At UCLA, we have investigated the efficacy as marker/reporter genes of HSV-TK enzymes identified for their increased toxicity with ACV and GCV [58]. We identified a mutated HSV1-TK enzyme (HSV1-sr39TK) that uses GCV and PCV substrates more effectively *and* TdR less effectively than the wild-type HSV1-TK enzyme. We created an adenovirus expressing this mutant HSV1-TK enzyme and demonstrated superior microPET imaging capabilities, with both FGCV and FPCV as PET reporter probes. Use of the HSV1-sr39TK enzyme and FPCV has improved the imaging capabilities of the HSV1-TK imaging system by an improvement in sensitivity of approximately two-fold. Additional studies with FHBG and HSV1-sr39tk show a further enhancement by a factor of ~2 in imaging sensitivity (unpublished data). The mutant enzymes offer the unique possibility of minimizing competition from substrates such as TdR that may be important for *in vivo* applications where intracellular TdR levels cannot be controlled. The approach of selecting mutant enzymes with enhanced affinity for a given marker/reporter probe should be applicable to various marker/reporter gene assays and should be a powerful general method to complement the search for alternate marker/reporter probes.

D2R Marker/Reporter Gene

The UCLA PET group has had a long interest in the striatal dopaminergic neurotransmitter system. A variety of positron-emitting probes for the dopamine biosynthetic, receptor and reuptake systems have been developed, both at UCLA and at other institutions. FESP, a positron-emitting analogue of the dopamine antagonist spiperone, was developed as a probe to image, by PET, D2R of the striatum [59]. Following intravenous (i.v.) injection of FESP, tissues rich in D2R bind and retain FESP. Thus, D2R-rich tissues can be imaged by PET scanning. Because 1) several high-specific activity PET probes, including FESP, already existed to image the D2R in living subjects [60] and 2) D2R expression is primarily restricted to the striatum, the UCLA gene imaging group has also developed the dopamine D2 receptor as a marker/reporter gene for *in vivo* reporter gene imaging, and FESP as the corresponding marker/reporter probe. The D2R/FESP and *HSV1-tk*/acycloguanosine systems for *in*

vivo imaging of marker/reporter gene expression have been developed at the same time at UCLA.

As described above for the *HSV1-tk* system, an adenovirus carrying the *D2R* gene driven by the CMV promoter (Ad-CMV-D2R) was used to image hepatic expression of D2R with FESP [61]. Mice were injected in the tail vein with Ad-CMV-βGal (serving as a control virus) or Ad-CMV-D2R. Two days later, the mice were injected through the tail vein with FESP and 3 hours later, imaged by microPET (Figure 12). Specific FESP signal is observed in the liver of the mouse injected with Ad-CMV-D2R; background signal is observed in the gastrointestinal tract and renal collecting system of both mice due to clearance of FESP from these routes.

To determine whether microPET can quantitatively monitor hepatic D2R expression in Ad-CMV-D2R infected mice, animals were injected with varying amounts of Ad-CMV-D2R virus, then injected with FESP and imaged by microPET. Hepatic FESP concentrations were determined by ROI analysis of the microPET scans [61]. After scanning, mice were killed and liver samples were analyzed for FESP retention by well counting and for functional D2R protein levels by [^{3}H]spiperone binding, using a conventional receptor binding assay. Fluorine-18 retained in liver, determined by ROI measurements of PET images of living mice, is proportional both to the amount of hepatic FESP present (well counting) and to hepatic D2R-dependent [^{3}H]spiperone binding; i.e., to D2R levels (Figure 13). *In vivo* PET analysis of hepatic D2R reporter gene expression accurately reflects *in vitro* determinations of D2R levels.

Imaging PET marker/reporter genes uses very small amounts of high-specific activity probes; the levels of PET imaging probes are typically orders of magnitude lower than the concentrations of the corresponding endogenous or pharmacologic agents required to elicit a biologic response. It is not the pharmacologic effect of FESP, which is administered at tracer levels, that is of concern in animals ectopically expressing the *D2R* gene, it is the response of these animals to endogenous ligands for the D2R. Ligand-activated D2R regulates intracellular cyclic adenosine monophosphate (cAMP) levels. Occupancy, by endogenous agonists, of ectopic D2R reporter might modulate the biology of target cells. Fortunately, D2R structure-function studies have identified amino acids that uncouple receptor occupancy from intracellular signaling [62–64]. Adenovirus strains with these D2R mutations are being developed, to compare PET imaging characteristics of functionally uncoupled and wild-type D2R.

Imaging of Both the *HSV1-tk* and D2R Marker/Reporter Genes in the Same Animal

Many applications may benefit from the ability to repetitively image two marker/reporter genes, expressed from distinct promoters, in the same living subject. To assess the feasibility of studying both the *HSV1-tk* and *D2R* reporter genes, the UCLA group has used a xenograft tumor model in nude mice to image these reporter genes with FPCV and
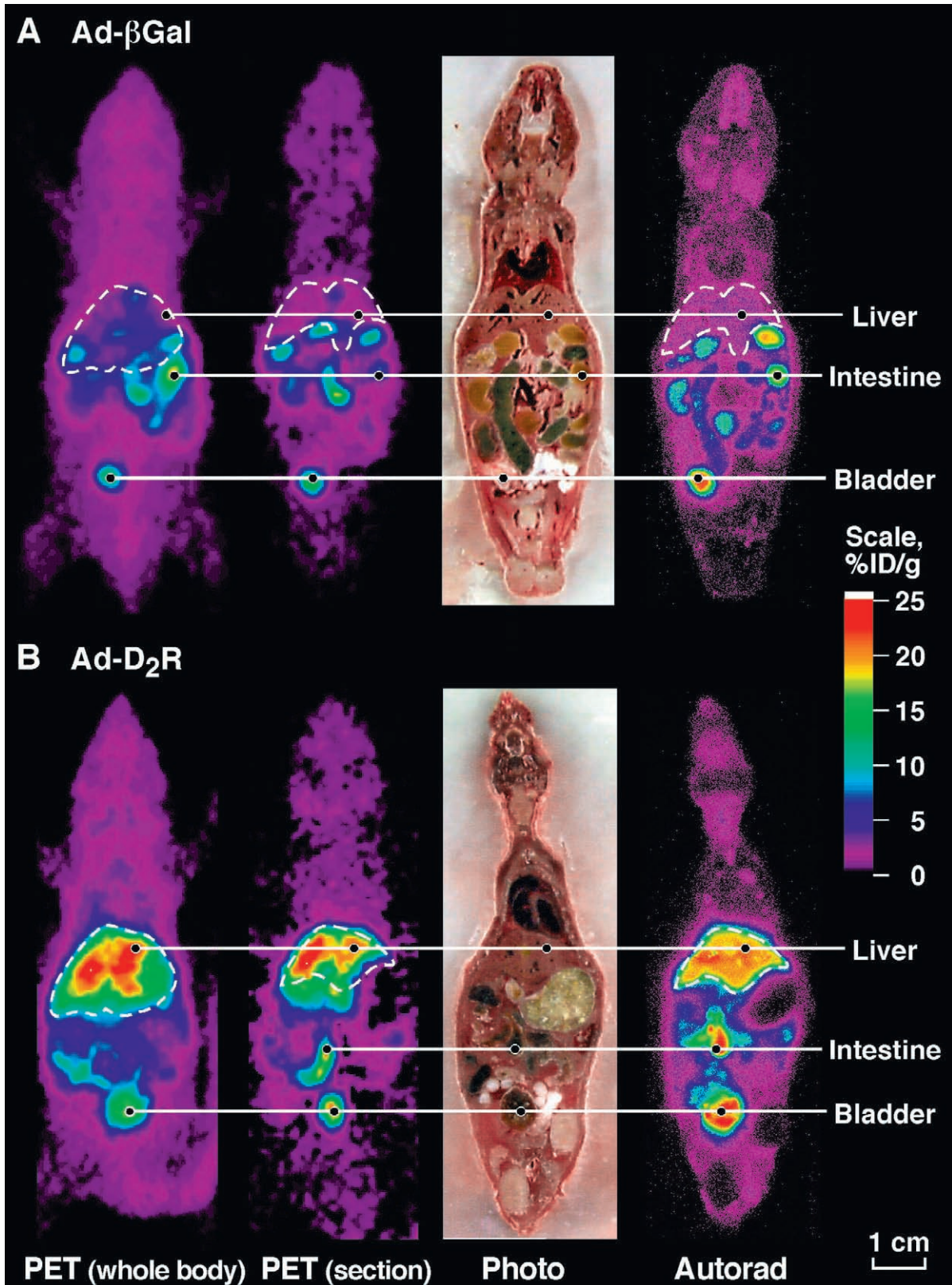
Figure 12. *PET and DWBA images of mice following Ad-CMV-βGal and Ad-CMV-D2R virus administration. Nude mice were injected through the tail vein with (A) 9×10^9 pfu of Ad-CMV-βGal virus or (B) 9×10^9 pfu of Ad-CMV-D2R virus. Two days after virus administration, both mice were injected through the tail vein with FESP (200 μCi, 200 μl). Three hours after the FESP injection, the animals were anesthetized, positioned supine with tail on left, and imaged with microPET. For each mouse, a whole body coronal projection image of the [^{18}F] activity distribution is displayed on the left. The liver outline, in white, was determined from both the FESP signal and cryostat slices. The second images from the left are coronal sections, approximately 2 mm thick, from the microPET. After their PET scans, the mice were killed, frozen and sectioned. The next images are photographs of the tissue sections (0.2 mm thick) corresponding to approximately the mid-thickness of the microPET coronal section. The images on the right are the DWBA (autorad) of these tissue sections. The color scale represents the %ID/g tissue. Images are displayed on the same quantitative color scale, to allow signal intensity comparisons among the panels.*
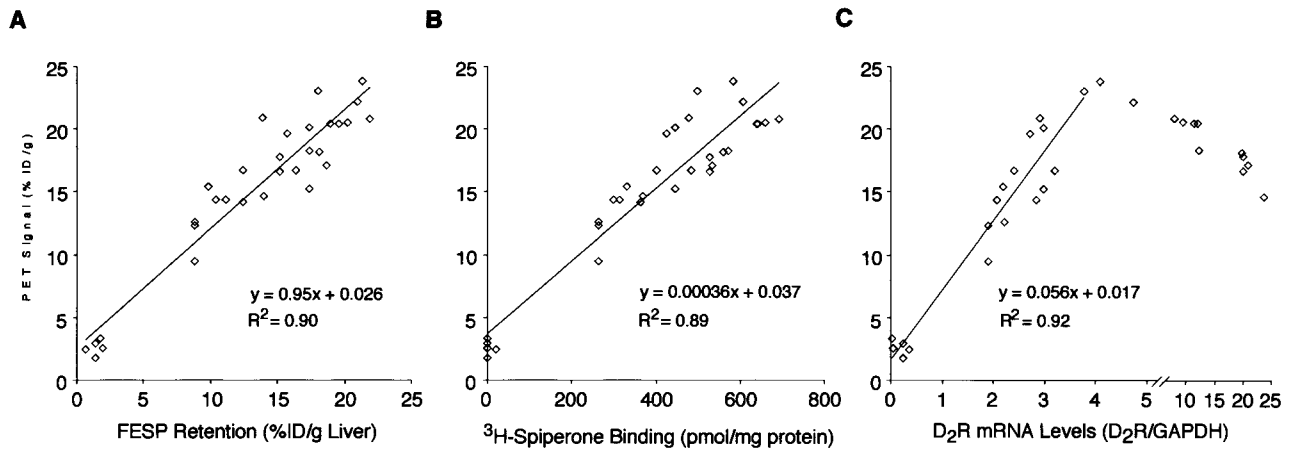
A

$y = 0.95x + 0.026$
$R^2 = 0.90$

PET Signal (% ID/g) — FESP Retention (%ID/g Liver)

B

$y = 0.00036x + 0.037$
$R^2 = 0.89$

^{3}H-Spiperone Binding (pmol/mg protein)

C

$y = 0.056x + 0.017$
$R^2 = 0.92$

D2R mRNA Levels (D2R/GAPDH)

Figure 13. *PET ROI analysis of images from living animals reflects hepatic FESP retention, D2R levels and D2R mRNA levels in Ad-CMV-D2R infected mice. Nude mice were injected through the tail vein with 5×10^6 to 9×10^9 pfu of Ad-CMV-D2R virus, to produce varying levels of D2R reporter gene expression. FESP was injected through the tail vein from 2 to 60 days after viral injection. Three hours after FESP injection, the mice were imaged in the ACAT PET scanner. The mice were then sacrificed, and their livers were removed and homogenized. Samples from each liver were analyzed for FESP and labeled FESP metabolites, [^{3}H]spiperone binding activity, and D2R mRNA and GAPDH mRNA levels. FESP metabolites were 1.0 ± 0.6 %ID/g liver. (A) In vivo hepatic [^{18}F] retention (measured by image analysis) as a function of in vitro hepatic FESP retention (measured by well counting). Note that the contribution of hepatic FESP metabolites has been removed from the values determined for FESP retention by well counting, but remain in the image data and contribute to a non-zero intercept. (B) In vivo analysis of hepatic [^{18}F] retention as a function of hepatic D2R levels, measured by [^{3}H]spiperone binding. (C) In vivo analysis of hepatic [^{18}F] retention as a function of GAPDH-normalized levels of hepatic D2R mRNA, measured by Northern blot analysis.*

FESP, respectively [65]. One nude adult mouse was implanted with 1×10^6 C6-stb-tk+ cells on the left shoulder and D2R+ cells [61] on the right shoulder. Tumors were allowed to grow for 10 days till they achieved a size of ~5^3 mm^3. The mouse was then injected with 150 μCi of FESP and imaged 2 hours later on a microPET scanner. Twenty-four hours later, the mouse was injected with 150 μCi of FPCV and again imaged 1 hour later on a microPET scanner (Figure 14). As expected, FESP and FPCV accumulate significantly only in the tumors with expression of D2R and *HSV1-tk*, respectively. Similar experiments have also been performed at UCLA using an adenoviral delivery model in which Ad-CMV-HSV1-tk and Ad-CMV-D2R are both injected in the same mouse followed by imaging with FPCV and FESP [65].

Animal Applications Utilizing Reporter Genes

Animal applications of the marker/reporter gene imaging assays are particularly important because they allow for the study of many important models in living animals. Fundamental questions in tumor biology can begin to be addressed with the techniques developed. Examples include: 1) "Tagging" tumor cells with a marker/reporter gene *ex vivo* so that the location of grafted tumor cells can be repetitively tracked in tumor cell trafficking studies. 2) Studying the interaction of the immune system with a given tumor type by using one reporter gene selectively expressed in a given subset of cells of the immune system (through appropriate choice of promoter), and by using a second reporter gene expressed only in tumor cells. The interaction of the tumor with the immune system can then be assessed over time by repeated imaging. 3) Quantitatively analyzing gene delivery to a given site (including tumors) by a variety of gene

delivery vectors. 4) Characterizing *in vivo* activation of gene deletion by imaging the activation of a marker/reporter gene concomitant with deletion of the gene of interest. 5) Characterizing interactions of tumor with stroma, following fundamental events such as neovascularization, by using a gene promoter specific for angiogenesis (e.g., vascular endothelial growth factor) coupled to the marker/reporter gene. In addition to problems in tumor biology, many areas of investigation including those related to developmental biology, teratology, adenoviral re-direction, cardiac angiogenesis, transplantation biology, etc. can all be significantly aided through the use of marker/reporter gene technology. In many of these applications, the ability to monitor the same animal over time without perturbing the underlying biology of the system offers unique possibilities only available only through non-invasive dynamic imaging techniques.

The use of transgenic animals carrying a marker/reporter gene offers unique possibilities for tracking a single animal repeatedly over time during experimental manipulations. Transgenic animals expressing the *HSV1-tk* gene from tissue-specific promoters have been developed to perform cell-specific ablation following administration of pharmacologic levels of pro-drugs such as GCV. A transgenic mouse model in which the *HSV1-tk* marker/reporter gene is driven by the albumin promoter has been studied at UCLA [66]. The albumin-*HSV1-tk* transgenic mice have been imaged on a microPET with both FPCV and FHBG and clearly demonstrate accumulation of marker/reporter probe in the mouse liver at 1 hour after injection. Restriction of reporter probe accumulation in the liver is the result of tissue-specific transcriptional activation of the HSV-tk marker/reporter gene by the albumin promoter (Figure 15). The albumin-*HSV1-tk* mice will be very useful for comparing alternate substrates *in vivo* and for assessing the reproducibility of

assays. As can be seen from Figure 15, the %ID/g liver in the albumin-HSV-tk transgenic mice is significantly higher with FHBG as reporter probe (8% to 11%) than with FPCV as reporter probe (3% to 6%). Studies are in progress to compare FHBG and [14C]FIAU in these transgenic mice using microPET and DWBA.

Advantages/Disadvantages of the Marker/Reporter Gene Assays Developed

The marker/reporter gene assays developed to date fall into the two main categories; enzyme-based (e.g., *HSV1-tk*) and receptor-based (e.g., D2R). Each of these assays has some distinct features that deserve special comment. An enzyme-based approach has the theoretical advantage of signal amplification, because one molecule of marker/reporter enzyme is capable of acting on many molecules of marker/reporter probes. A receptor-based assay such as the D2R system is capable of only a one-to-one stoichiometric interaction of marker/reporter ligand with receptor. For receptors that can be internalized and recycled, this one-to-one relationship may not be limiting. Enzyme-based approaches will always require intracellular transport of the marker/reporter substrate. This can be a confounding variable because rate of transport may change independent of levels of marker/reporter gene expression, thereby making it more difficult to quantitate the signal observed. Receptor-based approaches in which the receptor is primarily limited to the cell surface have the unique advantage of not requiring marker/reporter probe transport.

The *HSV1-tk* marker/reporter gene does not meet all the requirements of an ideal system. Expression of *HSV1-tk* may lead to an immune response, which is not optimal from the perspective of having an assay that will not perturb the normal cell environment. However, for transgenic animal studies in which the *HSV1-tk* gene is introduced into the first embryonic cell, an immune system response is not a confounding factor. In addition, male mice carrying *HSV1-tk* transgenes are frequently sterile; the result of a cryptic transcription start site that functions in the testes [67]. An additional limitation of the *HSV1-tk* system is that marker/reporter probes for this system do not significantly penetrate the intact blood-brain-barrier (BBB). Thus, for applications within the brain, methods to deliver the marker/reporter probe across the BBB and methods to facilitate exit of non-trapped probe must be developed.

The D2R marker/reporter gene also does not meet all the requirements of an ideal system. Because the D2R is expressed in mammalian tissue, there are no issues of an immune response. However, this same feature leads to a problem of background signal in the striatum where D2R is normally expressed. Continued development of marker/reporter genes and corresponding marker/reporter probes will be needed to produce more optimal assays. However, for many applications, the systems developed to date appear sufficiently robust.

"Direct" Marker/Reporter Transgene Imaging Strategies

Direct imaging strategies are based on imaging the transgene product directly. This can be achieved by "binding" of a radiolabeled ligand or probe directly to the gene product (e.g., mRNA, protein, receptor or epitope). As an example, some preliminary studies have been performed that use radiolabeled antisense probes to specifically hybridize to target mRNA *in vivo* (reviewed in Ref. [68]). Another approach involves amplification strategies, such as enzyme-specific trapping or transporter uptake of a radio-labeled probe. This latter approach was used in our initial studies described above [5,12,38,46,57,69] using *HSV1-tk* as a marker/reporter transgene (see Figure 1); we demonstrated that different radiolabeled probes are selectively phosphorylated and trapped in transduced cells expressing the gene product (enzyme) HSV1-TK.

The MSKCC group recently showed in an experimental animal model of colorectal hepatic metastasis that direct *HSV1-tk* imaging could be performed and used to evaluate adenoviral-mediated *HSV1-tk*-GCV gene therapy [70]. These imaging studies demonstrated two important points: 1) the ability to quantitatively assess the efficacy of intratumoral gene transfer and expression in a clinically relevant setting; 2) the ability to assess the specificity and safety of vector targeting by providing information (whole body images) about the location, magnitude and duration of *HSV1-tk* expression over time. An unexpected finding from these studies was the localization of *HSV1-tk* expression to small bile ducts when high doses of adenovirus were injected (based on quantitative autoradiographic FIAU images co-registered to histologic images obtained from the same tissue-liver section [70]). This observation probably explains the hepatotoxicity of adenoviral-mediated *HSV1-tk*-GCV gene therapy in this animal model when high doses of adenovirus are injected.

"Indirect" Marker/Reporter Transgene Imaging Strategies

Most therapeutic transgenes do *not* lend themselves to direct imaging of the transgene product. This is due to the fact that most therapeutic transgene products lack appropriate ligands or probes that can be radiolabeled and used to generate images that define the magnitude of transgene expression. In addition, it would be very time consuming and inefficient to develop and validate "new" ligands and probes for each therapeutic transgene. Alternatively, it is both feasible and reasonable to develop and validate "indirect" imaging strategies using a marker/reporter gene in combination with a therapeutic gene. Two strategies have been discussed: one strategy uses a fusion gene containing cDNA from both marker/reporter and therapeutic genes; the second strategy uses a *cis*-linked reporter gene (Figure 16). Both strategies are based on demonstrating a proportional and constant relationship in the co-expression of two transgenes over a wide range of expression levels. The advantage of this paradigm is that it can be applied to any gene combination. Strict co-expression of two proteins in equimolar amounts can only be achieved by a fusion gene encoding both gene products. This approach, however,
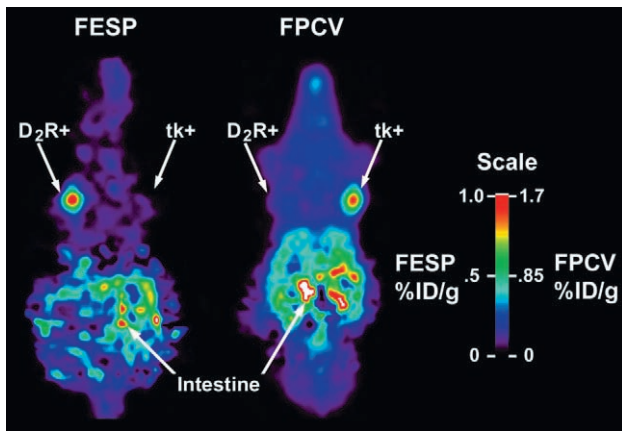
Figure 14. *D2R and HSV1‑tk tumor‑bearing mouse imaged on a microPET with FESP and FPCV. A nude mouse carrying a tumor that expresses D2R on the left shoulder and a tumor that expresses HSV1‑tk on the right shoulder was imaged on a microPET with FESP (day 0) and FPCV (day 1). Images are displayed using the same common global maximum. FESP accumulates primarily in the D2R positive tumor and FPCV accumulates primarily in the HSV1‑tk positive tumor. Background activity in the gastrointestinal tract is seen due to clearance of both FESP and FPCV from these routes. Renal clearance is not visible in the coronal sections shown.*

cannot be generalized as many fusion proteins may not yield functional activity or the fusion protein may not localize in the appropriate subcellular compartment. Fusion proteins may also induce an immunogenic reaction and, thus are, poorly suited for *in vivo* studies.

Both the MSKCC [71] and the UCLA [72] groups recently described and validated the proportional expression of two *cis*‑linked genes, using an IRES element within a single bicistronic transcription unit (Figure 16). These studies demonstrated that proportional co‑expression is reliable and quantitative in the context of *in vivo* imaging. The IRES element enables translation initiation within the bicistronic mRNA, thus permitting gene co‑expression by cap‑dependent translation of the first cistron and cap‑independent, IRES‑mediated translation of the second cistron [73–76].

The MSKCC group showed that the expression of *HSV1‑tk* using radiolabeled FIAU can be used to monitor the coordinated expression of *NTP cis*‑linked by the encephalomyocarditis virus (EMCV) IRES with the *HSV1‑tk* gene, following transduction with the SFG‑NIT retroviral vector [77]. The SFG‑NTP retroviral vector served as an *HSV1‑tk*‑negative control in these experiments. These vectors were used to transduce Jurkat cells *in vitro*. Several clones of transduced Jurkat cells were obtained and characterized for *NTP* surface marker gene expression using FACS analysis techniques. There was a linear relationship between the level of *NTP* expression on the cell surface and the level of *HSV1‑tk* gene expression (as measured by FIAU accumulation and sensitivity to GCV) in different clones of SFG‑NIT transduced Jurkat cells. These preliminary *in vitro* studies with an IRES‑based bicistronic NIT vector demonstrated that the *NTP* and *HSV1‑tk* genes are proportionally co‑expressed by transduced Jurkat cells, and this proportionality was maintained in all single‑cell clones tested and over a wide

range of gene expression levels. Furthermore, the level of *HSV1‑tk* gene expression in SFG‑NIT transduced Jurkat cell clones was within the range that is adequate for *in vivo* imaging, and suggests that similar multi‑gene expression cassette constructs could be useful for noninvasive monitoring of the homing sites, viability and proliferation of the transduced haematopoietic progenitor cells in patients.

The MSKCC group also showed that the expression of *HSV1‑tk* using radiolabeled FIAU and gamma camera imaging can be used to monitor the coordinated expression of the *Lac Z* gene in tumored animals [71,78]. A MoMVL‑based retroviral vector STLEO bearing *HSV1‑tk* and *Lac Z*/NeoR fusion genes linked by an IRES sequence was used to transduce RG2 and W256 tumor cells. Several single cell‑derived *in vitro* transduced clones were obtained by G418 selection. The level of *Lac Z* expression in different RG2STLEO and W256‑STLEO clones (and in tumors produced from the clones) was measured and directly compared with the FIAU radiotracer assay for *HSV1‑tk* gene co‑expression in the same clones (tumors). It was demonstrated that the expression of the two genes is proportional and constant in both *in vitro* and *in vivo* assays (Figure 17). It is important to note that the plots show results from the transduction of two different wild‑type cell lines (RG2 and W256 tumor cells) with different transduction efficiencies, yet the individual clones isolated from the bulk transduction culture and individual tumors generated from these clones fit along a single line. The observed correlation between the levels of *Lac Z* and *HSV1‑tk* gene expression, both *in vitro* and *in vivo*, demonstrates the potential for monitoring therapeutic gene
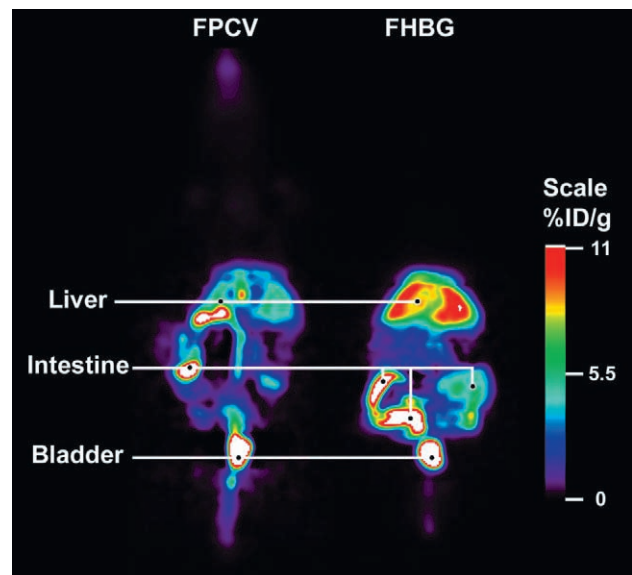

Figure 15. *FPCV and FHBG images of a transgenic mouse imaged with microPET. A transgenic mouse was studied in which the albumin promoter drives the HSV1‑tk marker/reporter gene. The mouse was imaged on day 0 with a microPET 1 hour after administration of FPCV (left panel) and on day 1 with FHBG (right panel). Both images are displayed using the same common global maximum and illustrate the higher %ID/g liver when utilizing FHBG compared with FPCV. There is significantly greater hepatic accumulation of FHBG compared to FPCV.*
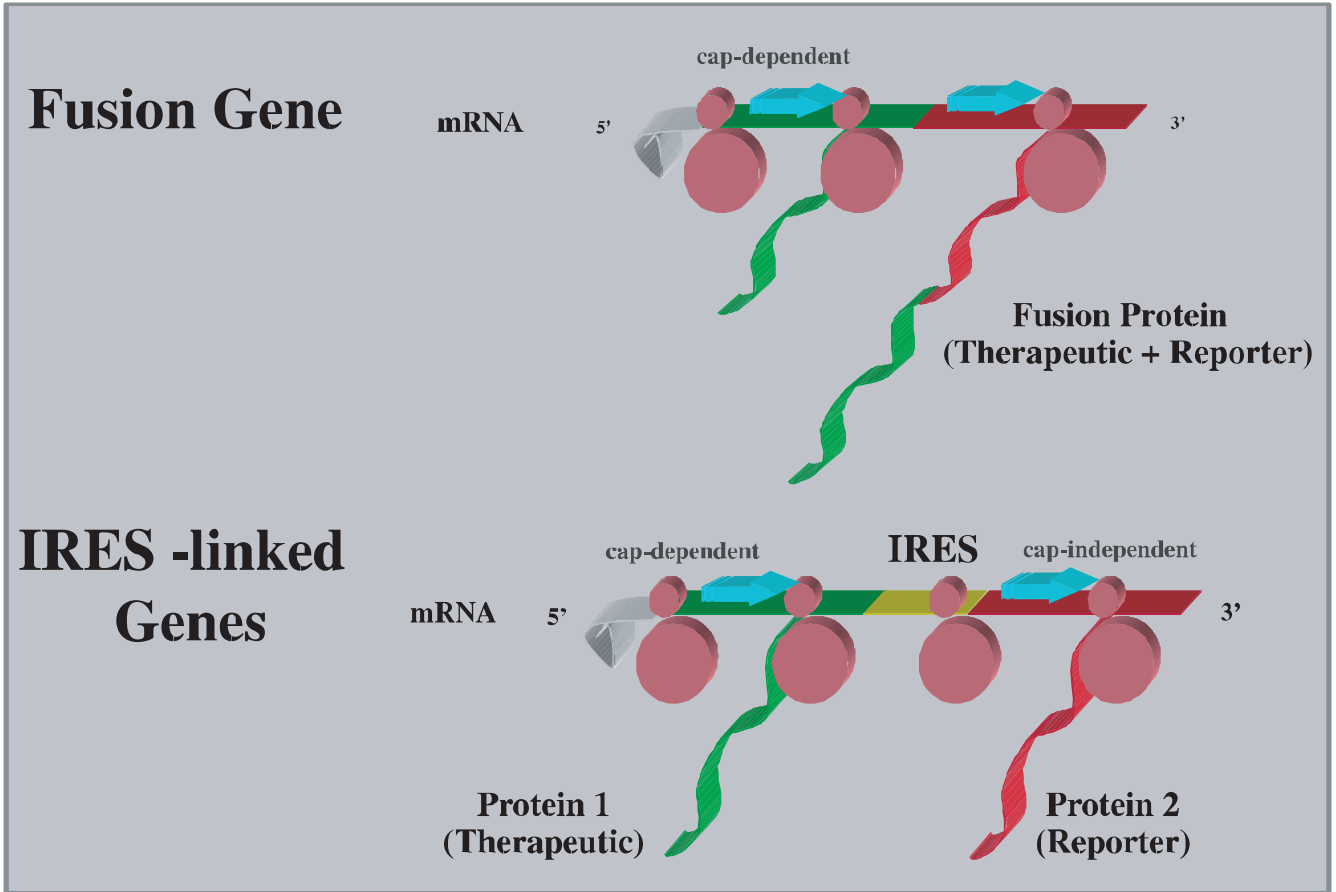
Figure 16. *Schematic of transgene co‑expression using fusion and internal ribosomal entry site (IRES)‑based strategies. In a fusion gene strategy, the mRNA is translated into a single fusion protein containing the therapeutic and reporter proteins. In the IRES‑linked gene strategy, the mRNA is translated into two distinct protein products through a cap‑dependent and cap‑independent process facilitated through the use of an IRES.*

transfer and expression by non‑invasive imaging of the *HSV1‑tk* marker/reporter gene.

The UCLA group has studied several constructs including pCMV‑RL‑IRES‑HSV1‑sr39tk, PCMV‑D2R‑IRES‑HSV1‑sr39tk and others to demonstrate correlated expression of the genes placed proximal and distal to a type II ECMV IRES [72]. Both in cell culture and in tumor‑bearing mice a correlation between expression of a "target gene" [renilla luciferase (RL) or the dopamine D2 receptor] and a PET marker/reporter gene [mutant HSV1‑tk, HSV1‑sr39tk] are observed. A high degree of correlation is obtained between the expression of target and marker/reporter genes both in stably transfected cells in culture using biochemical assays ($r^2 > 0.97$) and in tumor‑bearing mice ($r^2 > 0.90$) using microPET analysis with FPCV (for HSV1‑sr39tk expression) and FESP (for D2R expression) to image the expression of these reporter genes.

The imaging paradigms we describe above are not confined to one type of vector; the imaging paradigm can be extended to liposome‑encapsulated DNA, naked plasmid vectors, and other viral vectors, because IRES‑mediated co‑expression is determined at the translational level. Eventually, it will be important to assess if the IRES‑based vectors are reliable indicators of transgene co‑expression in different tissues, taking into account the half‑life of each encoded protein. These considerations will be important when using non‑invasive imaging to assess organ (tissue) specificity, as well as level and duration of transgene expression.

Potential Human Gene Therapy Applications

As noted in the Background section, a non‑invasive, clinically applicable method for imaging the expression of successful gene transduction in target tissue or specific organs of the body would be of considerable value. It would facilitate the monitoring and evaluation of gene therapy in human subjects by defining the *location*, *magnitude* and *persistence* of gene expression over time. Targeting gene therapy to particular tissue (e.g., tumor) or specific organs is an increasingly active area of research with 519 related articles published in 1991, 1424 articles in 1995, and 2499 articles in 1997 based on a MEDLINE search.

Several issues that are important for clinical optimization of gene therapy remain unresolved in many current clinical protocols: 1) Has gene transduction or transfection been successful?; 2) Is the distribution of the transduced or
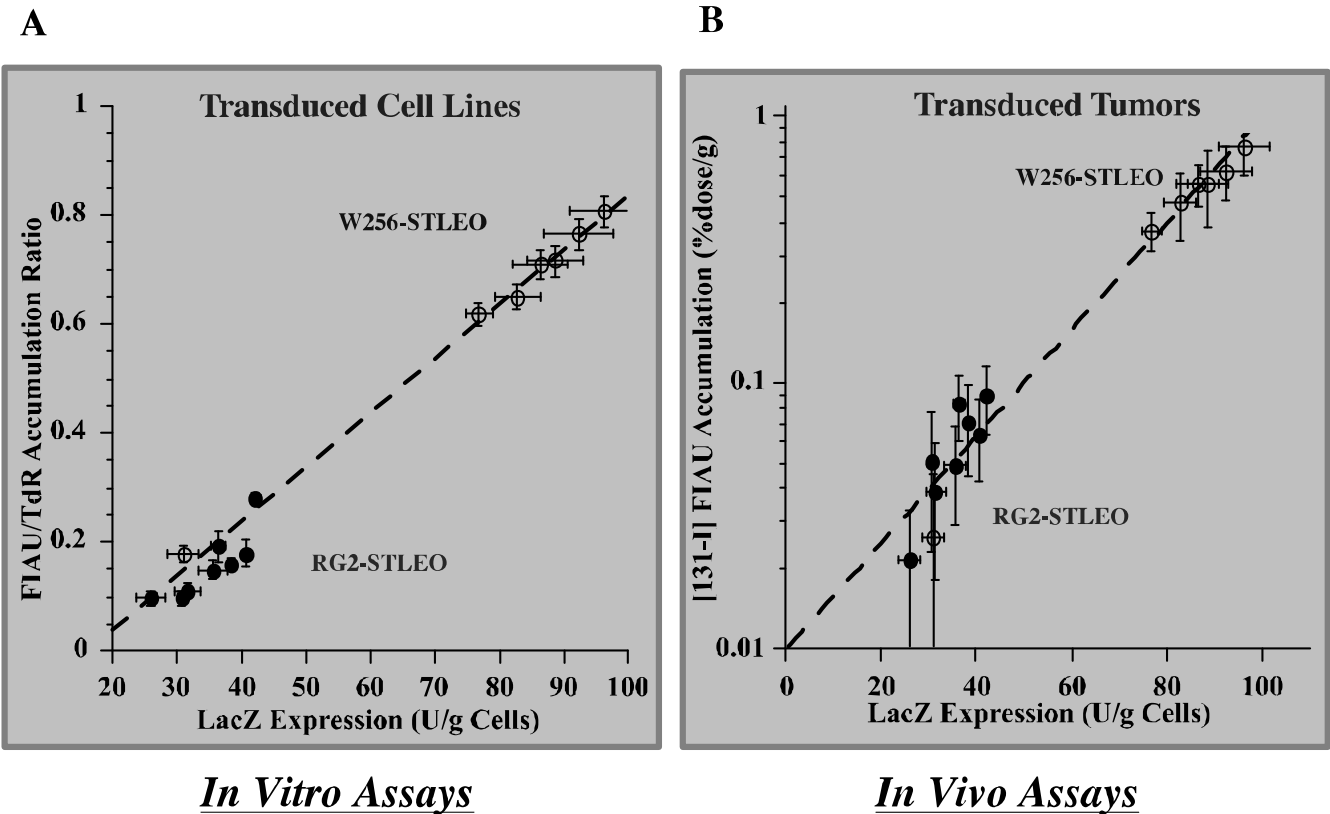
A

In Vitro Assays

B

In Vivo Assays

Figure 17. *IRES - mediated pseudo - bicistronic co - expression of HSV1 - tk and Lac Z genes. The MoMVL - based retroviral vector STLEO was used to stably transduce RG2 and W256 tumor cells. The level of Lac Z expression in different RG2 - STLEO and W256 - STLEO clones (and in tumors produced from the clones) were measured and directly compared with the FIAU radiotracer assay for HSV1 - tk gene co - expression in the same clones (tumors). A good correlation between the levels of Lac Z and HSV1 - tk gene expression was observed over a wide range of values in two separate cell lines with different transduction efficiencies, and this relationship was observed both in vitro ($y = -0.161 + 0.010x$, $r = 0.977$; left panel) and in vivo ($y = 0.010 \times e^{(0.046x)}$, $r = 0.995$; right panel).*

transfected gene localized to the target organ or to target tissue, and is the distribution in the target optimal?; 3) Is the level of transgene expression in the target organ or tissue sufficient to result in a therapeutic effect?; 4) Does the transduced or transfected gene localize to any organ or tissue at sufficient levels to induce unwanted toxicity?; 5) In the case of combined pro-drug-gene therapy protocols, when is transgene expression maximum (optimal) and when is the optimal time to initiate treatment with the pro-drug?; 6) How long does transgene expression persist in the target and other tissues?

We and others have proposed that noninvasive imaging techniques (including gamma camera, SPECT or PET) using selected marker/reporter gene and marker/reporter probe combinations will provide a practical and clinically useful way to identify successful gene transduction and expression in patients undergoing gene therapy, and that radiotracer imaging of transgene expression will be able to address the questions posed above. Although one could argue that biopsies of target tissue could be performed and that imaging is not critical, imaging provides some clear advantages. These include: 1) the ability to repeatedly assess gene expression that is very difficult using a biopsy approach, 2) the absence of any perturbation of the underlying tissue that occurs with biopsy procedures, and 3) a map of the entire body that provides an assessment not only of the target

organs (tissue), but other potential sites of gene expression as well, which could be important for toxicity issues.

Prospects for the Future
The primary applications of marker/reporter gene imaging *in vivo* are likely to be (i) repetitive, quantitative monitoring of the location, duration and extent of transgene expression, using bicistronic or fusion gene vectors that express therapeutic and reporter gene products from a common transcript and (ii) repetitive, quantitative evaluation of reporter gene expression over time in both patients and transgenic animals during longitudinal experiments. The advantages of high sensitivity, quantitative capability, and direct ability to translate the developed assays from animal to human studies will keep radionuclide-based approaches at the forefront of imaging gene expression.

References
[1] Culver KW, and Blaese RM (1994). Gene therapy for cancer. *Trends Genet* **10**, 174–178.
[2] Jolly D (1994). Viral vector systems for gene delivery. *Cancer Gene Ther* **1**, 51–64.
[3] List CP (1995). *Cancer Gene Ther* **2**, 225.
[4] Moolten FL (1986). Tumor chemosensitivity conferred by inserted herpes thymidine kinase genes: paradigm for prospective cancer control strategy. *Cancer Res* **46**, 5276–5281.

[5] Tjuvajev JG, Stockhammer G, Desai R, Uehara H, Watanabe H, Gansbacher B, and Blasberg RG (1995). Imaging the expression of transfected genes *in vivo*. *Cancer Res* **55**, 6126–6132.

[6] Gambhir SS, Barrio JR, Herschman HR, and Phelps ME (1999). Assays for noninvasive imaging of reporter gene expression. *Nucl Med Biol* **26**, 481–490.

[7] Contag PR, Olomu IN, Stevenson DK, and Contag CH (1998). Bioluminescent indicators in living mammals. *Nat Med* **4**, 245–247.

[8] Bogdanov A, and Weissleder R (1998). The development of *in vivo* imaging systems to study gene expression. *Trends Biotechnol* **16**, 5–10.

[9] Huang SC, and Phelps ME (1986). In *Positron Emission Tomography and Autoradiography, Principles and Applications for the Brain and Heart* (Chapter 7). Raven Press, New York.

[10] Weber DA, and Ivanovic M (1999). Ultra-high-resolution imaging of small animals: implications for preclinical and research studies. *J Nucl Cardiol* **6**, 332–344.

[11] Lear JL (1986). In *Principles of Single and Multiple Radionuclide Autoradiography*. Raven Press, New York.

[12] Gambhir SS, Barrio JR, Phelps ME, Iyer M, Namavari M, Satyamurthy N, Wu L, Green LA, Bauer E, MacLaren DC, Nguyen K, Berk AJ, Cherry SR, and Herschman HR (1999). Imaging adenoviral-directed reporter gene expression in living animals with positron emission tomography. *Proc Natl Acad Sci USA* **96**, 2333–2338.

[13] Kastis GK, Barber HB, Barrett HH, Gifford HC, Pang IW, Patton DD, Sain JD, Stevenson G, and Wilson DW (1998). High resolution SPECT imager for three-dimensional imaging of small animals (abstract) *J Nucl Med* **39**, 9 pp.

[14] Weber DA, and Ivanovic M (1995). Pinhole SPECT: ultra-high resolution imaging for small animal studies. *J Nucl Med* **36**, 2287–2289.

[15] Bloomfield PM, Rajeswaran S, Spinks TJ, Hume SP, Myers R, Ashworth S, Clifford KM, Jones WF, Byars LG, Young J, Andreaco M, Williams CW, Lammertsma AA, and Jones T (1995). The design and physical characteristics of a small animal positron emission tomograph. *Phys Med Biol* **40**, 1105–1126.

[16] Fricker RA, Torres EM, Hume SP, Myers R, Opacka-Juffrey J, Ashworth S, Brooks DJ, and Dunnett SB (1997). The effects of donor stage on the survival and function of embryonic striatal grafts in the adult rat brain: II. Correlation between positron emission tomography and reaching behaviour. *Neuroscience* **79**, 711–721.

[17] Hume SP, Lammertsma AA, Myers R, Rajeswaran S, Bloomfield PM, Ashworth S, Fricker RA, Torres EM, Watson I, and Jones T (1996). The potential of high-resolution positron emission tomography to monitor striatal dopaminergic function in rat models of disease. *J Neurosci Methods* **67**, 103–112.

[18] Cherry SR, Shao Y, Silverman RW, Meadors K, Siegel S, Chatziioannou A, Young JW, Jones WF, Moyers JC, Newport D, Boutefnouchet A, Farquhar TH, Andreaco M, Paulus MJ, Binkley DM, Nutt R, and Phelps ME (1997). MicroPET: a high resolution PET scanner for imaging small animals. *IEEE Trans Nucl Sci* **44**, 1161–1166.

[19] Jeavons AP, Chandler RA, and Dettmmar CAR (1999). A 3D HIDAC-PET camera with sub-millimetre resolution for imaging small animals. *IEEE Trans Nucl Sci* **46**, 468–473.

[20] Marriott CJ, Cadorette JE, Lecomete R, Scasnar V, Rousseau J, and van Lier JE (1994). High-resolution PET imaging and quantitation of pharmaceutical biodistributions in a small animal using avalance photodiode detectors. *J Nucl Med* **35**, 1390–1396.

[21] Weber S, Terstegge A, Herzon H, Reinartz R, Reinhart P, Rongen F, Muller-Gartner HW, and Halling H (1997). The design of an animal PET: flexible geometry for achieving optimal spatial resolution or high sensitivity. *IEEE Trans Med Imaging* **16**, 684–689.

[22] Fries O, Bradbury SM, Gebauer J, Holl I, Lorenz E, Renker D, and Ziegler SI (1997). A small animal PET prototype based on LSO crystals read out by avalanche photodiodes. *Nucl Instrum Methods* **A387**, 220–224.

[23] Chatziioannou AF, Cherry SR, Shao Y, Silverman RW, Meadors K, Farquhar TH, Pedarsani M, and Phelps ME (1999). Performance evaluation of microPET: a high resolution LSO PET scanner for animal imaging. *J Nucl Med* **40**, 1164–1175.

[24] Kinahan PE, and Rogers JG (1989). Analytic 3D image reconstruction using all detected events. *IEEE Trans Nucl Sci* **36**, 964–968.

[25] Qi J, Leahy RM, Cherry SR, Chatziioannou A, and Farquhar TH (1998). High-resolution 3D Bayesian image reconstruction using the microPET small-animal scanner. *Phys Med Biol* **43**, 1001–1013.

[26] Borrelli E, Heyman R, Hsi M, and Evans RM (1988). Targeting of an inducible toxic phenotype in animal cells. *Proc Natl Acad Sci USA* **85**, 7572–7576.

[27] Moolten FL, and Wells JM (1990). Curability of tumors bearing herpes thymidine kinase genes transfected by retroviral vectors. *J Natl Cancer Inst* **82**, 297–300.

[28] Culver KW, Ram Z, Walbridge S, Ishii H, Oldfield EH, and Blaise RM (1992). *In vivo* gene transfer with retroviral vector-producer cells for treatment of experimental brain tumors. *Science* **256**, 1550–1552.

[29] Moolten FL (1997). Suicide genes for cancer therapy. *Sci Med* **4**, 16–25.

[30] Iwashina T, Tovell DR, Xu LI, Tyrrell DL, Knaus EE, and Wiebe LI (1988). Synthesis and antiviral activity of IVFRU, a potential probe for non-invasive diagnosis of herpes simplex encephalitis. *Drug Res Delivery* **3**, 309–321.

[31] Saito Y, Price RW, Rottenberg DA, Fox JJ, Su T-L, Watanabe KA, and Philips FA (1982). Quantitative autoradiographic mapping of herpes simplex virus encephalitis with radiolabeled antiviral drug. *Science* **217**, 1151–1153.

[32] Saito Y, Rubenstein R, Price R, Fox JJ, and Watanabe KA (1984). Diagnostic imaging of herpes simplex virus encephalitis using antiviral drug: autoradiographic assessment in animal model. *Ann Neurol* **15**, 548–558.

[33] Price R, Cardle K, and Watanabe K (1983). The use of antiviral drugs to image herpes encephalitis. *Cancer Res* **43**, 3619–3627.

[34] Tovell D, Yacyshyn H, Misra H, Knaus EE, Wiebe LI, Samuel J, Gill MJ, and Tyrrell DL (1987). Effect of acyclovir on the uptake of ^{131}-I-labeled 5-iodo-2′-fluoro-2′-deoxy-1-β-D-arabino-furanosyl-uracil in herpes infected cells. *J Med Virol* **22**, 183–188.

[35] Blasberg RG, Gazendam J, Patlak CS, and Fenstenmacher JD (1980). Quantitative Autoradiographic Studies of Brain Edema and a Comparison of Multi-Isotope Autoradiographic Techniques. Raven Press, New York. pp. 255–270.

[36] Blasberg RG, Groothius D, and Molnar P (1981). Application of quantitative autoradiographic measurements in experimental brain tumor models. *Semin Neurol* **1**, 203–223.

[37] Tjuvajev JG, Finn R, Watanabe K, Joshi R, Oku T, Kennedy J, Beattie B, Koutcher J, Larson S, and Blasberg RG (1996). Noninvasive imaging of herpes virus thymidine kinase gene transfer and expression: a potential method for monitoring clinical gene therapy. *Cancer Res* **56**, 4087–4095.

[38] Tjuvajev JG, Avril N, Oku T, Sasajima T, Miyagawa T, Joshi R, Safer M, Beattie B, DiResta G, Daghighian F, Augensen F, Koutcher J, Zweit J, Humm J, Larson SM, Finn R, and Blasberg R (1998). Imaging herpes virus thymidine kinase gene transfer and expression by positron emission tomography. *Cancer Res* **58**, 4333–4341.

[39] Patlak CS, and Blasberg RG (1985). Graphical evaluation of blood-to-brain transfer constants from multiple-time uptake data. Generalizations. *J Cereb Blood Flow Metab* **5**, 584–590.

[40] Patlak CS, Blasberg RG, and Fenstermacher JD (1983). Graphical evaluation of blood-to-brain transfer constants from multiple-time uptake data. *J Cereb Blood Flow Metab* **3**, 1–7.

[41] McKenzie R, Fried MW, Sallie R, Conjeevaram H, Di Bisceglie AM, Park Y, Savarese B, Kleiner D, Tsokos M, Luciano C, Pruett T, Stotka JL, Straus SE, and Hoofnagle JH (1995). Hepatic failure and lactic acidosis due to fialuridine (FIAU), and investigational nucleoside analogue for chronic hepatitis B. *N Engl J Med* **333**, 1099–1105.

[42] Misra HK, Knaus EE, Wiebe LI, and Tyrell DL (1986). Synthesis of ^{131}I, ^{125}I, ^{123}I and ^{82}Br labelled 5-halo-1-(2-deoxy-2-fluoro-*b*-D-arabinofuranosyl) uracils. *Appl Radiat Isot* **37**, 901–905.

[43] Balatoni JA, Finn RD, Tjuvajev JG, Larson SM, and Blasberg RG (1997). Synthesis and quality assurance of radioiodinated 2′-fluoro-2′-deoxy-1-*b*-D-arabinofuranosyl-5-[*I]iodo-uracil. *J Labelled Compd Radiopharm* **40**, 103.

[44] Manning FJ, and Swartz M (1995). Review of Fialurdine (FIAU) Clinical Trials. Institute of Medicine, Washington, DC.

[45] Blasberg R, and Tjuvajev J (1997). *In Vivo* Monitoring of Gene Therapy by Radiotracer Imaging. In *Ernst Shering Research Foundation Workshop 22: impact of molecular biology and new technical developments on diagnostic imaging*. Springer Verlag, Berlin-Heidelberg. pp. 161–189.

[46] Gambhir SS, Barrio J, Wu L, Iyer M, Namavari M, Satyamurthy N, Bauer E, Parrish C, MacLaren D, Borghei A, Berk A, Cherry S, Phelps ME, and Herschman H (1998). Imaging of adenoviral directed herpes simplex virus type 1 thymidine kinase gene expression in mice with ganciclovir. *J Nucl Med* **39**, 2003–2011.

[47] Srinivasan A, Gambhir SS, Green LA, Cherry SR, Sharfstein S, Barrio JR, Satyamurthy N, Namavari M, Wu L, Berk AJ, Phelps ME, and Herschman H (1996). A PET reporter gene (PRG)/PET reporter probe (PRP) technology for repeatedly imaging gene expression in living animals. *J Nucl Med* **37**, 107 p.

[48] Barrio JB, Namavari M, Phelps ME, and Satyamurthy N (1996). Regioselective fluorination of substituted guanines with dilute F2: a facile entry of 8-fluoroguanine derivatives. *J Org Chem* **61**, 6084–6085.

[49] Namavari M, Barrio JR, Gambir SS, Cherry SR, Herschman HR, Phelps ME, and Satyamurthy N (in press). Synthesis of 8-[^{18}F] fluoroguanine derivatives: in-vivo probes imaging gene expression with PET. *Nucl Med Biol*.

[50] Gambhir SS, Barrio JR, Bauer E, Iyer M, Namavari M, Satyamurthy N, Shah P, Toyokuni T, Wu L, Berk AJ, Phelps ME, and Herschman H (1998). Radiolabeled penciclovir: a new reporter probe with improved imaging properties over ganciclovir for imaging herpes-simplex virus type 1 thymidine kinase reporter gene expression (abstract). *J Nucl Med* **39**, 53 p.

[51] Boyd MR, Safrin S, and Kern ER (1993). Penciclovir: a review of its spectrum of activity, selectivity, and cross-resistance pattern. *Antiviral Chem Chemother* **4**, 3–11.

[52] Monclus M, Luxen A, Cool V, Damhaut P, Velu T, and Goldman S (1997). Development of a positron emission tomography radio-pharmaceutical for imaging thymidine kinase gene expression: synthesis and in vitro evaluation of 9-{(3-[^{18}F]Fluoro-1-hydroxy-2-propoxy)methyl}guanine. *Bioorg Med Chem Lett* **7**, 1879–1882.

[53] Alauddin MM, Conti PS, Mazza SM, Hamzeh FM, and Lever JR (1996). Synthesis of 9-[(3-[^{18}F]fluoro-1-hydroxy-2-propoxy)methyl]guanine ([^{18}F]FHPG): a potential imaging agent of viral infection and gene therapy using PET. *Nucl Med Biol* **23**, 787–792.

[54] Alauddin MM, and Conti PS (1998). Synthesis and preliminary evaluation of 9-(4-[^{18}F]-fluoro-3-hydroxymethylbutyl)guanine ([^{18}F]FHBG): a new potential imaging agent for viral infection and gene therapy using PET. *Nucl Med Biol* **25**, 175–180.

[55] Bading JR, Alauddin MM, Fissekis JD, Kirkman E, Raman RK, and Conti PS (1997). Pharmacokinetics of F-18 fluorohydroxy-propoxymethylguanine (FHPG). *J Nucl Med* **38**, 43 p.

[56] Green LA, Gambhir SS, Barrio JR, Bauer E, Nguyen K, Namavari M, Cherry SR, Herschman H, and Phelps ME (1998). Tracer kinetic modeling of 8-(F18)-fluoroganciclovir PET data: a new tracer for measuring reporter gene expression. *J Nucl Med* **39** (suppl), 10 p.

[57] Gambhir SS, Bauer E, Black M, Liang Q, Kokoris MS, Barrio JR, Iyer M, Namavari M, Satyamurthy N, Green LA, Nguyen K, Cherry SR, Phelps ME, and Herschman HR (in press). A mutant herpes simplex virus type 1 thymidine kinase reporter gene shows improved sensitivity for imaging reporter gene expression with positron emission tomography. *Proc Natl Acad Sci USA*.

[58] Black ME, Newcomb TG, Wilson H-MP, and Loeb LA (1996). Creation of drug-specific herpes simplex virus type 1 thymidine kinase mutant for gene therapy. *Proc Natl Acad Sci USA* **93**, 3525–3529.

[59] Barrio JB, Satyamurthy N, Huang SC, Keen R, Nissenson CHK, Hoffman JM, Ackermann RF, Bahn MM, Mazziotta JC, and Phelps ME (1989). 3-(2'-[^{18}F]fluoroethyl)spiperone: in vivo biochemical and kinetic characterization in rodents, nonhuman primates, and humans. *J Cereb Blood Flow Metab* **9**, 830–839.

[60] Satyamurthy N, Barrio JR, Bida GT, Huang S, Mazziotta JC, and Phelps ME (1990). 3-(2'-[^{18}F]fluoroethyl)spiperone, a potent dopamine antagonist: synthesis, structural analysis and in vivo utilization in human. *Appl Radiat Isot* **41**, 113–129.

[61] MacLaren DC, Gambhir SS, Satyamurthy N, Barrio JR, Sharfstein S, Toyokuni T, Wu L, Berk AJ, Cherry SR, Phelps ME, and Herschman HR (1999). Repetitive, non-invasive imaging of the dopamine D2 receptor as a reporter gene in living animals. *Gene Ther* **6**, 785–791.

[62] Neve KA, Cox BA, Henningsen RA, Spanoyannis A, and Neve RL (1991). Pivotal role for aspartate-80 in the regulation of dopamine D2 receptor affinity for drugs and inhibition of adenylyl cyclase. *Mol Pharmacol* **39**, 733–739.

[63] Cox BA, Henningsen RA, Spanoyannis A, Neve RL, and Neve KA (1992). Contributions of conserved serine residues to the interactions of ligands with dopamine D2 receptors. *J Neurochem* **59**, 627–635.

[64] Woodward R, Roley C, Daniell S, Naylor LH, and Strange PG (1996). Investigation of the role of conserved serine residues in the long form of the rat D2 dopamine receptor using site-directed mutagenesis. *J Neurochem* **66**, 394–402.

[65] Gambhir SS, MacLaren DC, Barrio JR, Toyokuni T, Satyamurthy N, Nguyen K, Berk A, Wu L, Cherry SR, Phelps ME, and Herschman HR (1999). Noninvasive and Repeated Imaging of Reporter Gene Expression in Living Mice Utilizing Positron Emission Tomography. American Society of Gene Therapy, Washington, DC.

[66] Herschman HR, MacLaren DC, Satyamurthy N, Barrio JR, Sharfstein S, Green LA, Iyer M, Namavari M, Toyokuni T, Wu L, Berk AJ, Cherry SR, Phelps ME, Sandgren EP, and Gambhir SS (in press). Seeing is believing: non-invasive, quantitative and repetitive imaging of reporter gene expression in living animals, using positron emission tomography. *J Neurosci Res*.

[67] Braun RE, Lo D, Pinkert CA, Widera G, Flavell RA, Palmiter RD, and Brinster RL (1990). Infertility in male transgenic mice: disruption of sperm development by HSV-tk expression in postmeiotic germ cells. *Biol Reprod* **43**, 684–693.

[68] Gambhir SS, Barrio JR, Herschman HR, and Phelps ME (1999). Imaging gene expression: principles and assays. *J Nucl Cardiol* **6**, 219–233.

[69] Tjuvajev JG, Joshi R, Lindsley L, Balatoni J, Finn R, Larson S, Sadelain M, and Blasberg R (1998). Noninvasive imaging of HSV1-tk marker gene with FIAU for monitoring transfer and expression of other therapeutic genes by multi-gene delivery vectors. *J Nucl Med* **39**, 130 p.

[70] Tjuvajev JG, Chen SH, Joshi A, Joshi R, Guo ZS, Balatoni J, Ballon D, Koutcher J, Finn R, Woo SL, and Blasberg RG (1999). Imaging adenoviral-mediated herpes virus thymidine kinase gene transfer expression in vivo. *Cancer Res* **59**, 5186–5193.

[71] Tjuvajev J, Joshi A, Callegari J, Lindsley L, Joshi R, Balatoni J, Finn R, Larson S, Sadelain M, and Blasberg R (1999). A general approach to the non-invasive imaging of transgenes using cis-linked herpes simplex virus thymidine kinase. *Neoplasia* **1**, 315–320.

[72] Yu Y, Annala AJ, Barrio JR, Toyokuni T, Satyamurthy N, Namavari M, Cherry SR, Phelps ME, Herschman HR, and Gambhir SS (in press). Quantitation of target gene expression by imaging reporter gene expression in living animals. *Nat Med*.

[73] Pelletier S (1988). Internal initiation of translation of eukaryotic mRNA directed by a sequence derived from poliovirus RNA. *Nature* **334**, 320.

[74] Jackson RJ, and Kaminski A (1995). Internal initiation of translation in eukaryotes: the picornovirus paradigm and beyond. *RNA* **1985**.

[75] Sachs AB, Sarnow P, and Hentze MW (1997). Starting at the beginning, middle, and end: translation initiation in eukaryotes. *Cell* **89**, 831–838.

[76] Ghattas SAM (1991). The encephalomyocarditis virus internal ribosomal entry site allows efficient coexpression of two genes from a recombinant provirus in cultured cells and in embryos. *Mol Cell Biol* **11**, 5848.

[77] Tjuvajev JG, Gallardo H, Joshi A, Joshi R, Blasberg R, and Sadelain M (1997). Bi-cistronic co-expression of a cell surface marker gene and the HSV-tk gene in jurkat cells: implications for noninvasive imaging in vivo. *Cancer Gene Ther* **4**, S44.

[78] Tjuvajev JG, Avril N, Lindsley L, Safer M, Joshi R, Beattie B, Larson S, Sadelain M, and Blasberg R (1997). Monitoring the expression of therapeutic genes by noninvasive imaging of the HSV1-tk marker gene using double-gene vector constructs. *Cancer Gene Ther* **4**, S43–S44.